Schweizerische Eidgenossenschaft
Confédération suisse
Confederazione Svizzera
Confederaziun svizra

Federal Department of the Environment, Transport, Energy and Communications DETEC

Swiss Federal Office of Energy SFOE
Energy Research and Cleantech Division

REEL Demo – Romande Energie ELectric network in local balance Demonstrator

Deliverable: 5d3 A list of possible ancillary services for enhanced grid operation and implementation of the most effective ones at the RE demo site

Demo site: Rolle

Developed by
Lionel BLOCH (EPFL-PVlab)
Luc GIRARDIN (EPFL-IPESE)
Jordan HOLWEGER (EPFL-PVlab)
Luise MIDDELHAUVE (EPFL-IPESE)
In collaboration with
Romande Energie (RE)

[Sion/Neuchâtel, 27.06.2020]

Contents

Nomenclature

ACRONYMS

AS	Ancillary services
BES	Building energy system
CAPEX	Capital Expenditure
DHW	Domestic hot water
DSM	Demand Side Management
DSO	Distribution System Operators
ERA	Energy reference area
GM	Grid multiple
GU	Grid usage
LV	Low Voltage
MILP	Mixed integer linear programming
MPC	Model Predictive Control
MV	Medium Voltage
OPEX	Operational Expense
PV	Photovoltaic
PVC	Grid curtailment
RBC	Rule-Based Approach
REel Demo	Romande Energie ELectric network Demonstrator
SC	Self-consumption
SOFC	Solid Oxide Fuel Cells
SS	Self-sufficiency

Executive summary

There is a need by distribution system operators and power suppliers to propose ancillary services to enhanced grid operation allowing the optimal deployment of photovoltaic panels, cogeneration technologies and distributed storage. This deliverable therefore proposes and evaluates the impact of a list of possible ancillary services for the injection of local renewable energy in the future low voltage grid.

The novelty of the proposed building to district and district to grid approaches lies in the ability to generate a wide range of optimal energy transition scenarios using multi-objective optimisation techniques both at building and district level. The proposed approach differs from previous work by integrating ancillary services by optimizing simultaneously both sizing and operation of the district energy technologies.

This deliverable demonstrates, on the reference case (TR3716), the implementation of voltage control ancillary services to integrate more renewable energy to the low voltage grid. In particular it exposes how advanced electricity tariffs can influence energy system design and operation to decrease stress induced by high PV penetration on the grid. The proposed implementation can be deployed in control boxes developed using open-source standards, such as mikrobus.

Moreover, considering the transformer's area as a relevant scale for the implementation of ancillary services, this work pave the way to the definition of a new geographical division for territorial energy planning aiming at the integration more renewable energy resources in urban areas.

1. Description of deliverable and goal

1.1. Introduction

According to the International Renewable Energy Agency, the share of clean district energy systems for building heat demand is projected to more than double by 2050 with a significant increase by 70% of the electricity demand in the sector [17]. The decarbonization of the energy resources employed would indeed require large-scale electrification of the thermal utilities, combined with investments in efficient renewable technologies. The path toward this goal is not straightforward as the emergence of new decentralized electricity production, distributed storage, and new consumers are going to put more pressure on the electrical grid, especially at the district level. For instance, the electricity demand in the building sector is expected to increase by 70% by 2050, highlighting the importance to strategically plan the interaction between households with electricity power grid. Namely, voltage deviation, line and transformer overloading are key issues that need to be addressed.

For these reasons, there is a need by DSO's and power suppliers to propose ancillary services to enhanced grid operation (Figure 1) allowing the optimal deployment of photovoltaic panels (PV), cogeneration technologies and distributed storage.

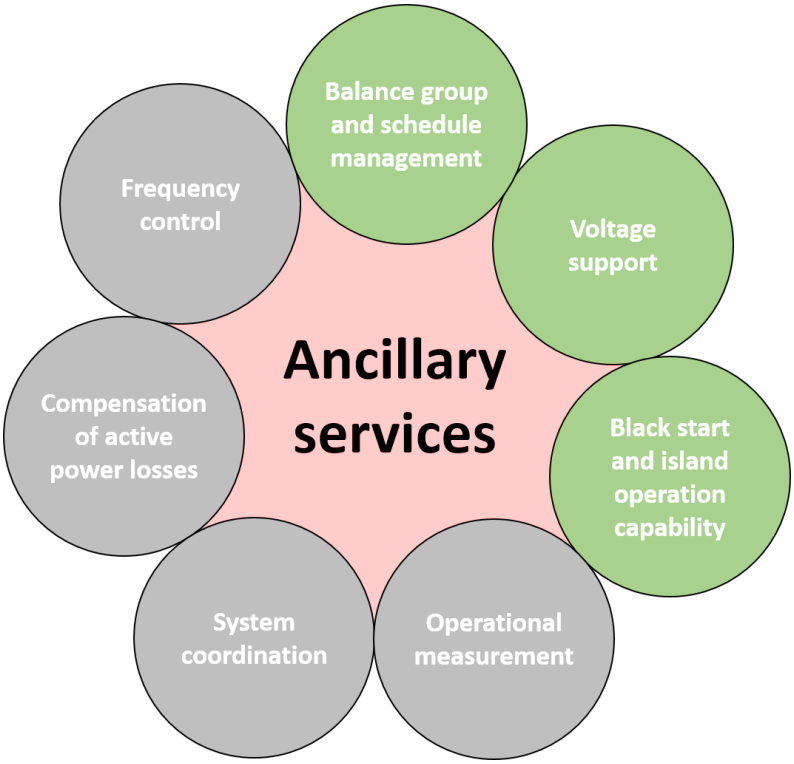

Figure 1: Overview of ancillary services defined by swissgrid [15].
The one addressed in this report ate shown in green.

Starting from the actual electricity load and energy-mix at the transformers (Figure 2), the report evaluates the effect of energy scheduling, voltage support and island operation measures on the low voltage grid when more photovoltaic panels (PV), batteries, heat pumps and cogeneration are integrated.

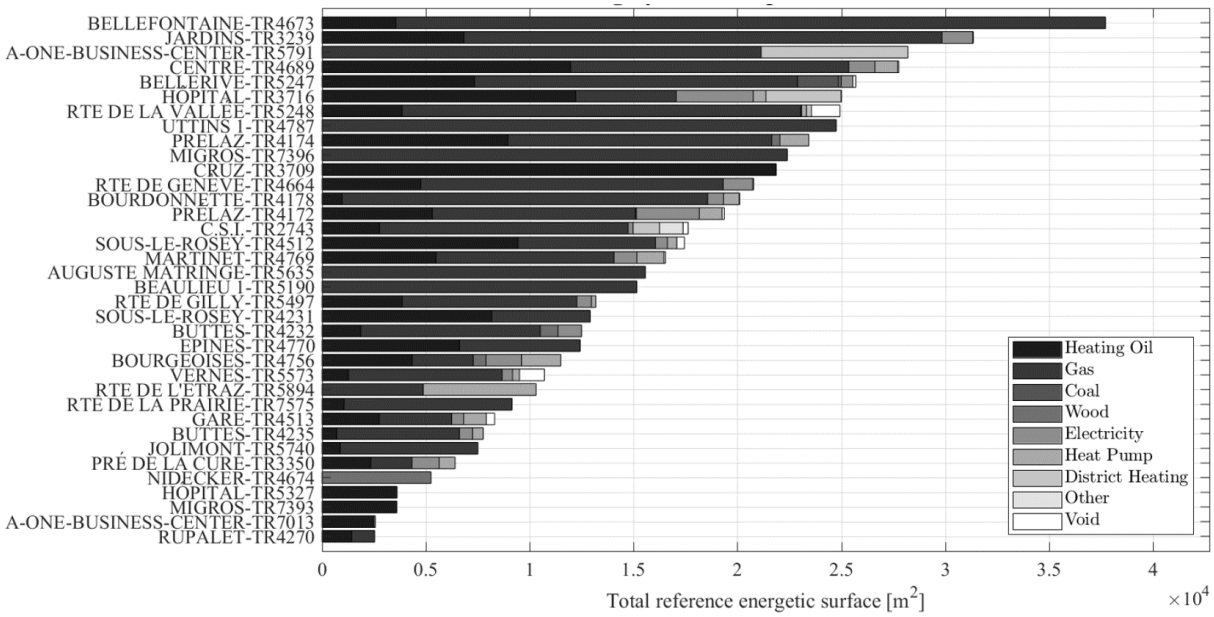

Figure 2: Actual heat-energy mix of the transformers [3].

1.2. Research question

The increasing penetration of renewable energy in the RE Demo site through the integration of new PV capacity [1] and the shift from fossil fuel to heat pumps leads to the following practical question:

- what are the possible ancillary services to enhance the future operation of the power grid at district scale;
- what is the impact, at the level of the transformer, of the implementation of the most effective ancillary services.

1.3. Novelty of the proposed solutions compared to the state-of-art

Recent investigations [26] within the field of smart Building energy system management have highlighted the use of optimal and predictive control methods as a good candidate to perform ancillary services such as load shifting and peak shaving [9]. However, most studies solely focused on the development of detailed control algorithms [7, 4] with a limited set of empirically defined [35] or fixed [25, 32] system configurations. The same stands for the increasing interest by power network operators to provide load flexibility through demand-side-management [13, 14, 40].
On the other hand, grid impact assessment has attracted interest from the research community due to the rapid growth of distributed renewable energy. Solving the load flow problem has shown that, in the presence of distributed power generation, the topology of the network has a great importance on the risk of voltage rise [39]. Moreover, as shown by [6], battery energy storage, PV curtailment, reactive power control and on load tap changer drastically improves the maximum PV penetration.

The novelty of the proposed building to district and district to grid approaches lies in the ability to generate a wide range of optimal energy transition scenarios using multi-objective optimisation techniques both at building and district level. This allows to access the impact of ancillary service provision in an early design phase. In this context, grid impact assessment not only used to access the maximum voltage level in a sub-network [28], but rather to evaluate the power flow for the yearly operation of various energy system configurations, thus allowing to evaluate ancillary services as a function of the evolution of the grid.

Our approach to integrate ancillary services from DSM differs from previous work by considering the optimization of both the sizing of the PV and battery system and its operation using a fully integrated formulation contrary to a two-step optimization as in [37]. Compared to the

[1] https://jardinsolaire.ch/projet

latter, our approach ensures a global optimum of the net present value but take into account neither PV degradation nor the consumption evolution. In comparison to [8], we choose a finer temporal resolution (15 min), which is closer to the recommendation of [1, 5] for modeling variable renewable energy sources. Additionally, we integrate more-advanced tariff structures, inspired by [30], but considering their impact on the system configurations while adding a real-time pricing energy tariff. In addition to the standard performance metric to assess the usage of the grid such as maximum peak power, self-consumption and self-sufficiency [31, 29, 19], we consider another grid usage metric which compares the maximum power exported or imported with the maximum load power.

1.4. Description of the deliverable

In the first chapter, the future loads in the low voltage grid are forecasted as a function of technology scenarios in buildings (§3.2). In order to solve overloading issues, possible ancillary services are reviewed (§3.3) and a list of the most effective one are proposed for the RE Demo site (§3.4). This includes the effect of implementing the proposed ancillary services is then evaluated at the level of the transformer TR3716 of the reference case study of the RE Demo site (figure 3).

The impact on the grid is assessed by solving the load-flow problem and evaluating voltage deviations, line loading levels and the load duration curve at the transformer. This includes the implementation of different tariff structures (§3.5), the use of model predictive control (MPC) (§4.4), the application of load constraints in the power grid §4.5 and district rather than building scale control (§4.6).

Our results show that future technology mix increases grid congestion but enable new economic models for flexibility services.

Figure 3: Transformer in the RE Demo zone (triangles) with TR3716 within the references case area (magenta).

2. Achievement of Deliverable

2.1. Date

This deliverable is handed in June 2020.

2.2. Demonstration of the Deliverable

This deliverable demonstrates on the reference case (TR3716) the implementation of voltage control ancillary services to integrate more renewable energy to the low voltage grid. In particular it exposes how advanced electricity tariffs can influence energy system design and operation to decrease stress induced by high PV penetration on the grid.

2.3. Impact

Starting from the demonstration on the reference case of REel, the proposed control strategies provides solution for the operation of future districts in Switzerland integrating solar energy, heat pumps, cogeneration with new storage capacities. It capitalizes on the local flexibility by giving incentives from advanced tariffs to use as much as possible locally produced renewable energy without relying on centrally controlled infrastructures.

3. Research methodology

The implementation of the proposed methods have been demonstrated on the low voltage grid connected to the transformer TR3716 of the RE Demonstrator(Figure 4).

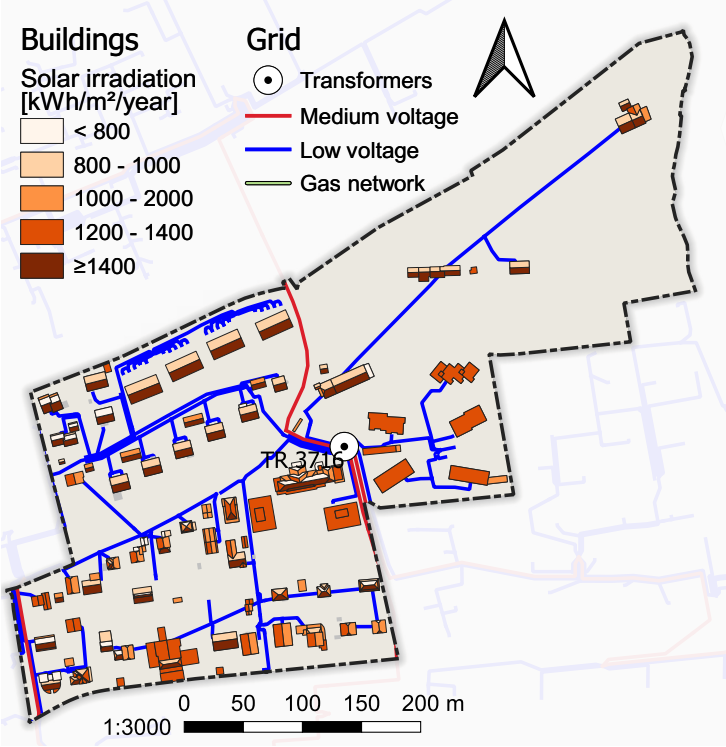

Figure 4: Low voltage grid TR3716 of the RE Demonstrator.

3.1. Actual loads on the low voltage grid

The actual load at the transformer, obtained from DEPSYS measurements, is shown in Figure5. The power capacity of this transformer is limited to ±400 KW.

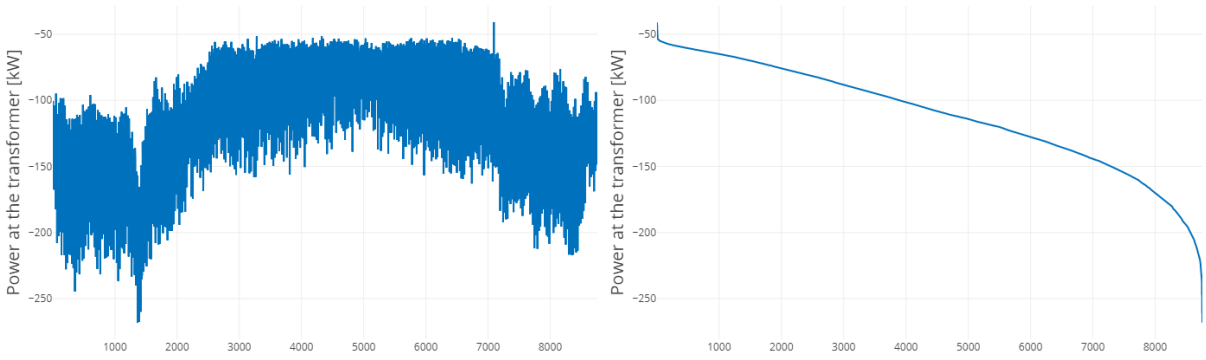

(a) Power profile. *(b) Load duration curve.*

Figure 5: Actual measurement (2018) at the transformer TR3716 (source: Depsys).

3.2. Future loads on the low voltage grid

The future loads on the low voltage grid is evaluated using the approach developed in the project [20] for the elaboration of alternative scenarios of the future building energy system (BES). It uses a MILP-based optimization model [34, 26] to design and schedule the operation of smart buildings by minimizing the operational costs (*OPEX*) as a function of capital investment (*CAPEX*) bounds (ϵ). Scenarios at district scale (s) are generated by selecting energy system scenario for buildings ($s_{b,i}$) taken from a pre-defined list of optimal combination of state-of-the-art technologies listed in Table 1.

Table 1: Bounds for the sizes of the building energy system

Technology		Min	Max
Heat pump	kW_e	1.5	-
Boiler	kW_e	0.1	-
PV	kW_p	0.5	-
Battery	kWh	0.1	100
Thermal storage (heating)	m^3	0.1	10
Thermal storage (DHW)	m^3	0.06	10
Electrical heater (backup heating)	kW_{th}	0	100
Electrical heater (backup DHW)	kW_{th}	0	100
SOFC	kW_e	0.7	2.5

The generation of N scenarios at district scale is obtained by choosing, for each building (b), the set of scenario ($s_{b,i}$) minimising the operating cost of Equation 1 under the ϵ-constraint of Equation 2.

$$OPEX_{s,j} = \min_{b,i} \sum_{b,s} OPEX_{b,s_{b,i}} \tag{1}$$

$$CAPEX_{s,j} = \sum_{b,i} CAPEX_{b,s_{b,i}} \leq \epsilon_j,\ j \in [1,..,N] \tag{2}$$

The electricity demand ($\dot{E}_d$) is decomposed into the import from the grid ($\dot{E}_{imp}$), export to the grid ($\dot{E}_{exp}$), self-generated electricity ($\dot{E}_{sg} = \dot{E}_{PV} + \dot{E}_{SOFC}$) and battery losses ($\dot{E}_{loss}$) according to the electricity balance of Equation 3 and Figure6.

$$\dot{E}_d = \dot{E}_{imp} + \dot{E}_{sg} - \dot{E}_{exp} - \dot{E}_{loss} \tag{3}$$

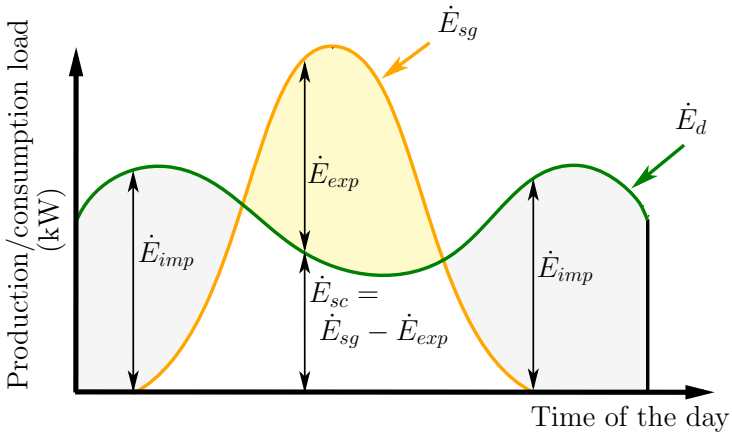

Figure 6: Schematic outline of daily net load ($\dot{E}_{sg} - \dot{E}_{exp} + \dot{E}_{imp}$), net generation ($\dot{E}_{sg}$) and absolute self-consumption ($\dot{E}_{sg} - \dot{E}_{exp}$).

The self-consumption (SC) and self-sufficiency (SS) indicators [22, 26] defined by Equation 4. respectively 5, are reported as well in the secondary axis of the plot.
It is worth to notice that island operation capability ($SS = 1$) is limited by the available PV potential on the roof of buildings and by the maximum size imposed to battery (100 kWh) and SOFC (2.5 kW_e) for each individual house.

$$SC = \frac{\dot{E}_{sg} - \dot{E}_{exp}}{\dot{E}_{sg}} \tag{4}$$

$$SS = \frac{\dot{E}_{sg} - \dot{E}_{exp}}{\dot{E}_{sg} - \dot{E}_{exp} + \dot{E}_{imp}} \tag{5}$$

Load at the transformer

The load at the transformer ($\dot{E}_T^j$) of Equation 6 is obtained by summing up the electrical loads of the global optimal configuration (j) formed by a unique scenario ($s_{b,j}$) for each building (b).

$$\dot{E}_T^j = \sum_b \dot{E}_{imp}^{b,s_{b,j}} + \dot{E}_{exp}^{b,s_{b,j}} \tag{6}$$

Three possible load constraint in the power grid have been implemented to avoid overloading: grid multiple (GM), grid usage (GU) and PV curtailment (PVC) [24].

1. Grid Multiple The GM limits the peak power of the grid to the average demand of a period [26]. Equation 7 defines the grid multiple, where p_d is the total period duration.

$$\epsilon_{GM} \geq \frac{\left(\dot{\boldsymbol{E}}^{\boldsymbol{gr},+}_{\boldsymbol{p,t}} - \dot{\boldsymbol{E}}^{\boldsymbol{gr},-}_{\boldsymbol{p,t}}\right)}{\frac{1}{p_d}\sum_t \left(\dot{\boldsymbol{E}}^{\boldsymbol{gr},+}_{\boldsymbol{p,t}} - \dot{\boldsymbol{E}}^{\boldsymbol{gr},-}_{\boldsymbol{p,t}}\right)} \quad \forall p \in P \quad \forall t \in T \tag{7}$$

2. Grid Usage The GU gives the interaction with the grid in respect to the maximum uncontrollable load of the building. This is excluding heating as it is to evaluate the impact of a total system design on the grid. Equation 8 defines the GU according to [16].

$$\epsilon^{+/-}_{GU} \geq \frac{\dot{\boldsymbol{E}}^{\boldsymbol{gr},+/-}_{\boldsymbol{p,t}}}{\max\limits_{p,t}(\dot{E}^{b,-}_{p,t})} \quad \forall p \in P \quad \forall t \in T \tag{8}$$

3. PV curtailment The PVC factor presented in Equation 9 is the ratio between the total amount of PV energy hat is curtailed from the PV generation [16].

$$PVC = \frac{\boldsymbol{E}^{\boldsymbol{pv}}_{\boldsymbol{g}}\boldsymbol{en} - E^{pv}_{sc}}{\boldsymbol{E}^{\boldsymbol{PV,gen}}} \tag{9}$$

3.3. Possible ancillary services for the low voltage grid

Definition and classification

The term ancillary services (AS) is widely used in the context of power system stability; however, according to the author, its definition can differ. It usually refers to services that help to corrective measures used to maintain the voltage and frequency of the power grid in a secure range. Table 2 shows a few definitions of the AS term, Swissgrid [36] considers that AS are provided only by the grid operator where as the directive 2009/72/EC [41] incorporates ”all services necessary for the operation of a transmission or distribution system”. Moreover [10] makes the distinction between ancillary services and system services. ”System services are all services provided by some system function (such as a system operator or a grid/network operator) to users connected to the system. Ancillary services are services procured by a system functionality (system operator or grid/network operator) from system users in order to be able to provide system services.”

Table 2: Ancillary services definitions

Reference	Definition
Swissgrid [36]	... operating a reliable grid requires constant corrections. The corrective measures **taken by the grid operators** are referred to as “ancillary services”. Ancillary services **maintain the frequency and the voltage** within a secure, stable range and compensate for the difference between electricity production and consumption. Ancillary services include schedule and congestion management as well as the provision of control energy.
Joos [18]	Services provided in addition to real power generation by the electric utilities under a monopoly, and services that must be provided separately under a deregulated environment.
EURELECTRIC [10]	All services required by the transmission or distribution system operator to enable them to maintain the integrity and stability of the transmission or distribution system as well as the power quality.
Directive 2009/72/EC [41]	All services necessary for the operation of a transmission or distribution system.

Systems can provide one or multiple kind of ancillary services listed in table 3.

Table 3: Ancillary services kind according to [27] and [10]

Name	Definition
Primary frequency control (FC1)	Local **automatic control** that adjusts the active power generation of the generating units and the consumption of controllable loads to restore quickly the balance between load and generation and counteract frequency variations.
Secondary frequency control (FC2)	**Centralized automatic control** that adjusts the active power production of the generating units to restore the frequency and the interchanges with other systems to their target values following an imbalance.
Tertiary frequency control (FC3)	**Manual changes** in the dispatching and commitment of generating units.
Primary voltage control (VC1)	Local **automatic control** that maintains the voltage at a given bus at its set point.
Secondary voltage control (VC2)	**Centralized automatic control** that coordinates the actions of local regulators in order to manage the injection of reactive power within a regional voltage zone.
Tertiary voltage control (VC3)	**Manual optimization** of the reactive power flows across the power system.
Black start capability (BS)	The capability of a generating unit to **start up without an external power supply**, called on as a means of restoring supplies following a major failure on all or part of the network.
Remote automatic generation control (RG)	A means of regulating frequency by controlling the output through a centrally-based control system. It can mean operating the Secondary Response but also controlling a whole plant.
Grid loss compensation (GL)	Compensating the transmission system losses between the generators and the loads.
Emergency control actions (EC)	Maintenance and use of special equipment (e.g. power-system stabilisers and dynamic-braking resistors) to maintain a secure transmission system.

3.4. Most effective ancillary services for the RE demo site

According to the building to district[2] (Task 1.1) and district to grid[3] (Task 1.2) approach with time steps ranging from 15 minutes up to 1 hour, the following primary (VC1) and secondary (VC2) voltage control ancillary services are considered the most effective for the low voltage grid of the district:

- Advanced electricity tariff structures §3.5 and §4.3;
- Model predictive control (MPC) §4.4;
- Load constraints in the power grid §4.5;
- Building to district control §4.6.

3.5. Alternative electricity tariffs

This section briefly summarizes the equations of the optimization problem, defines the performance metrics for the design and operation of all buildings, and presents the performance metrics from the grid perspective.

PV-battery optimal sizing and operation

The PV and battery sizing and operation are optimized for each building to minimize the total cost of ownership given a set of modeling constraints [2]. The objective function includes both the investment and operational cost, as described in (10). By definition, the optimization problem relies on the assumption that an exact forecast of both the PV generation and the electrical load is provided. The impact of forecast errors and energy managers' performance is outside the scope of this study. In the following, P denotes a power, C a cost and L a duration. The complete definitions of all variables are available in [2].

$$\mathsf{obj} = \frac{r \cdot (1+r)^L}{(1+r)^L - 1} \cdot \left(\mathsf{CX}_{\mathsf{pv}} + \frac{L}{L^{\mathsf{BAT}}} \cdot \mathsf{CX}_{\mathsf{bat}} \right) + \mathit{OPEX} \tag{10}$$

$$\mathsf{CX}_{\mathsf{pv}} = \sum_{i=1}^{N} n_i^{\mathsf{MOD}} \cdot P_{\mathsf{nom},i}^{\mathsf{MOD}} \cdot C_i^{\mathsf{MOD}} + b^{\mathsf{PV}} \cdot \mathsf{CF}^{\mathsf{PV}} \tag{11}$$

$$\mathsf{CX}_{\mathsf{bat}} = E_{\mathsf{CAP}}^{\mathsf{BAT}} \cdot C^{\mathsf{BAT}} + b^{\mathsf{BAT}} \cdot C_F^{\mathsf{BAT}} \tag{12}$$

[2]Building to district (Task 1.1): Exploration of system design options to increase the flexibility of the energy system by optimizing building efficiency together with multi-energy systems

[3]District to grid (Task 1.2): Enhancement of grid operation by designing district-level multi-energy systems capable of providing flexibility to the power system

where the decision variables are the number of PV modules installed n_i^{MOD} for each configuration, and the battery size $E_{\text{CAP}}^{\text{BAT}}$. The boolean variables $b^{\text{PV}}, b^{\text{BAT}}$ are constrained to switch from 0 to 1 if the corresponding capacity is greater than 0.

The operation decision variables are the battery charging and discharging power ($P_t^{\text{CHA,DIS}}$) and the PV curtailment (P_t^{CUR}). These decision variables determine the power withdrawn from - injected to - the grid ($P_t^{\text{IMP}}, P_t^{\text{EXP}}$) through the conservation of energy (13):

$$\begin{aligned} P_t^{\text{IMP}} - P_t^{\text{EXP}} - P_t^{\text{CHA}} + P_t^{\text{DIS}} - P_t^{\text{CUR}} + P_t^{\text{PV}} \\ = P_t^{\text{LOAD}} \quad \forall t \in T \end{aligned} \tag{13}$$

where $P_t^{\text{PV}} = \sum_{i=1}^{N} P_{t,i}^{\text{MOD}} \cdot n_i^{\text{MOD}}$ in which $P_{t,i}^{\text{MOD}}$ is the power generated by a single module of the i^{th} configuration at time t.

Then, the operating cost *OPEX* (14a) can be evaluated, considering the sum of the grid exchange cost $\text{OX}_{\text{ge}}^{\text{st}}$ according to the selected tariff structure, i.e. volumetric (14c), capacity (14d), or block rate (14e). The operating cost also contains the PV maintenance cost OX_{pm} as defined in (14b).

Op. cost
$$\textit{OPEX} = \sum_{st}^{[vol,pow,block]} \text{OX}_{\text{ge}}^{\text{st}} + \text{OX}_{\text{pm}} \tag{14a}$$

PV maint.
$$\text{OX}_{\text{pm}} = \gamma^{PV} \cdot \text{CX}_{\text{pv}} \tag{14b}$$

Volumetric
$$\text{OX}_{\text{ge}}^{\text{vol}} = \sum_{t=1}^{T} [P_t^{\text{IMP}} \cdot t_t^{\text{IMP}} - P_t^{\text{EXP}} \cdot t_t^{\text{EXP}}] \cdot \text{TS}_t \tag{14c}$$

Capacity
$$\text{OX}_{\text{ge}}^{\text{pow}} = \sum_{m=1}^{M} P_m^{\text{MAX}} \cdot t^{\text{MAX}} \tag{14d}$$

Block rate
$$\begin{aligned} \text{OX}_{\text{ge}}^{\text{block}} = & \sum_{t=1}^{T} \max_{k=1\ldots K} (P_t^{\text{IMP}} \cdot a_k^{\text{IMP}} \cdot \text{TS}_t + b_k^{\text{IMP}}) \\ & - \sum_{t=1}^{T} \min_{k=1\ldots K} (P_t^{\text{EXP}} \cdot a_k^{\text{EXP}} \cdot \text{TS}_t + b_k^{\text{EXP}}) \end{aligned} \tag{14e}$$

where the maximum power for month m, P_m^{MAX}, is calculated by requiring that both the import and the export power be smaller than this variable.

The five tariff scenarios are illustrated in figure 7. The values of the import and export tariff $t_t^{\text{IMP}}, t_t^{\text{EXP}}$, the value of the capacity tariff t^{MAX} and the values of the block rate tariff coefficients $a_k^{\text{IMP}}, a_k^{\text{EXP}}$ are given in Table 4. The values of the coefficients b_k^{IMP} and b_k^{EXP} are calculated to ensure the continuity of the cost of buying or selling energy to the grid (see Fig. 7). All other variables from (10) to (14a) which are known parameters of the optimization problem are defined in Table 5.

Table 4: Tariff scenarios

Scenario	Description	Tariff (CHF cts/kWh)	
reference	t_t^{IMP}:	21.02	
	t_t^{EXP}:	8.16	
solar	$t_{t\in 11h:15h}^{\text{IMP}}$:	14.68	
	$t_{t\in 11h:15h}^{\text{EXP}}$:	7.07	
	$t_{t\notin 11h:15h}^{\text{IMP}}$:	23.17	
	$t_{t\notin 11h:15h}^{\text{EXP}}$:	11.12	
spot market	t_t^{IMP}:	EPEX*3.9468	
	t_t^{EXP}:	EPEX*1.604	
capacity	t_t^{IMP}:	15.91	
	t_t^{EXP}:	12.09	
	t^{MAX}:	5.02 CHF/kW/month	
block rate	Power (kW)	a_k^{IMP}	a_k^{EXP}
	0 to 1	13.72	13.07
	1 to 2	15.06	11.73
	2 to 4	16.80	9.99
	4 to 6	19.07	7.73
	6 to 8	22.01	4.79
	8 to 10	25.83	0.96

Table 5: Parameters

	Parameter	Value	Description
GENERAL	T	35040	number of time steps
	M	12	number of months
	TS	900 s	time steps
	L	25 years	system lifetime
	r	3%	discount rate
PV	$P_{\text{CAP,max},b}^{\text{PV}}$	*	maximum building PV capacity
	C_F^{PV}	10049 CHF	PV fixed cost **
	C^{PV}	1.05 CHF/W	PV specific costs **
BAT	C^{BAT}	229 CHF/kWh	battery specific cost **
	C_F^{BAT}	0 CHF	battery fixed cost **

* data from the geographical information system

** same value for all buildings

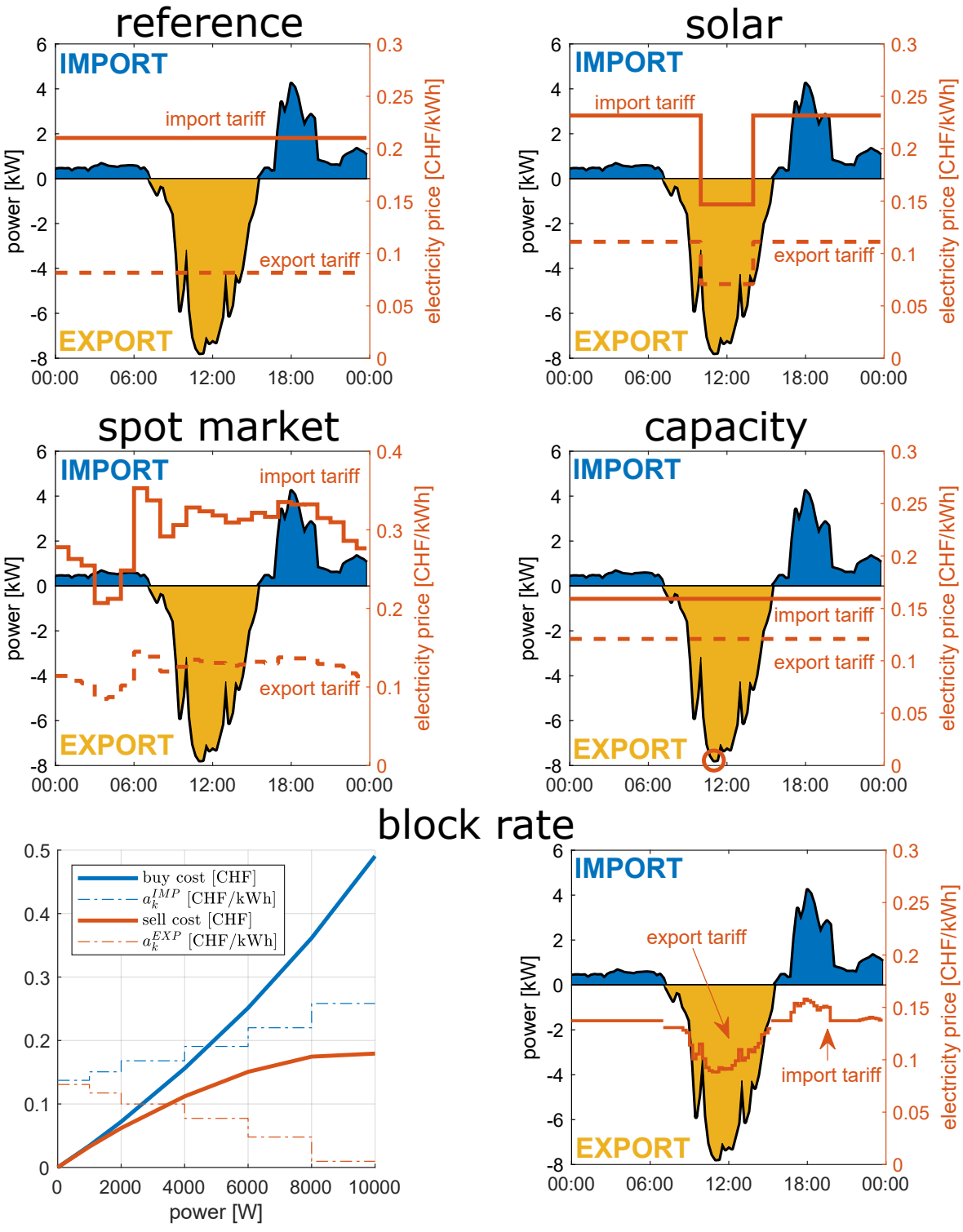

Figure 7: Scenario preview for a typical day with PV generation.

Performance metrics

The performance metrics aim to assess the system's reaction, in terms of equipment size and operation, and the network's reaction, in terms of voltage profile and line loading, when chang-

ing the electricity pricing structure. From a design perspective, the PV host (15a) is the ratio between the installed PV capacity and the maximum PV potential capacity of the building. The PV penetration (15b) compares the energy generated by the PV arrays with the annual consumption. The battery autonomy ratio, BAT auto (15c), corresponds to the ratio between the battery capacity and the mean daily consumption of the building. This metric can be understood as the fraction of a day that can be covered by the battery in the event of a blackout. From an operation perspective, the PV cur (15d) is the fraction of the energy that is curtailed from the PV generation. The self-sufficiency SS (15i) is the fraction of the energy consumption that is self-covered by the PV-battery system. The definition of (15i) is derived from [21]. To assess how the buildings interact with the grid, we defined in [2] a grid usage ratio, GU IMP,EXP 15e, as the ratio between the maximum withdrawn/injected power and the maximum load. Finally, from an economic perspective, the payback period, DPP (15g), (time to recover the investment) is of crucial interest to evaluate the profitability of the proposed economic framework. The levelized cost of energy (LCOE (15h)) also helps to assess whether the chosen scenario induces an increase or a decrease in the electricity price.

$$\text{PV host} = \text{PV}^{\text{CAP}} / \text{PV}^{\text{CAP}}_{\text{max}} \tag{15a}$$

$$\text{PV penetration} = \sum_t P_t^{\text{PV}} / \sum_t P_t^{\text{LOAD}} \tag{15b}$$

$$\text{BAT auto} = \frac{E^{\text{BAT}}_{\text{CAP}}}{\text{mean daily energy}} \tag{15c}$$

$$\text{PV cur} = \sum_t P_t^{\text{CUR}} / \sum_t P_t^{\text{PV}} \tag{15d}$$

$$\text{GU IMP,EXP} = \max(P_t^{\text{IMP,EXP}}) / \max(P_t^{\text{LOAD}}) \tag{15e}$$

$$\text{NPV} = \sum_{t=1}^{L} \text{CF}_t / (1+r)^t \tag{15f}$$

$$\text{DPP} = T \mid \frac{\sum_{t=1}^{T} \text{CF}_t - \mathit{OPEX}_t^0}{(1+r)^t} = 0 \tag{15g}$$

$$\text{LCOE} = \frac{\text{NPV}}{L \cdot \sum_t P_t^{\text{LOAD}} \cdot TS_t} \tag{15h}$$

$$\text{SS} = \frac{\sum_t \min(P_t^{\text{LOAD}}, P_t^{\text{EXP}} + P_t^{\text{LOAD}} - P_t^{\text{IMP}})}{\sum_t P_t^{\text{LOAD}}} \tag{15i}$$

where CF_t is the net cash flow (investment + maintenance cost + operational cost, including battery replacement) at time t and OPEX_t^0 is the original operating cost without the investment in the PV and battery.

The resolution of the power-flow equations allows for extracting the voltage (in per unit, p.u) at

every node of the network and the current flowing through every line. Given the lines' properties, in particular, the maximum allowable current, a representative metric for grid congestion is the line loading level. In addition, the maximum and minimum voltage magnitude at every injection bus will be studied. This allows us to distinguish when there is a local excess of energy from when there is a local deficit of energy. Finally, one of the key issues for the high penetration of distributed stochastic generators is the reverse-power flow occurring at the link between the low-voltage side and the upper level. For this reason, the load duration curve enables us to assess the requirement in terms of power that has to flowed into and out of the low-voltage grid.

4. Results

4.1. Future loads at the transformer

The future loads have been computed and aggregated using the methodology defined in section 3.2.

Figures 8 and 9 shows the annual operation and investment cost of equipment per square meter of energy reference area (ERA) at district scale for 28 optimal scenarios. Scenarios 1-14 are generated without considering cogeneration while scenarios 15-28 integrate the cogeneration with SOFC in buildings.

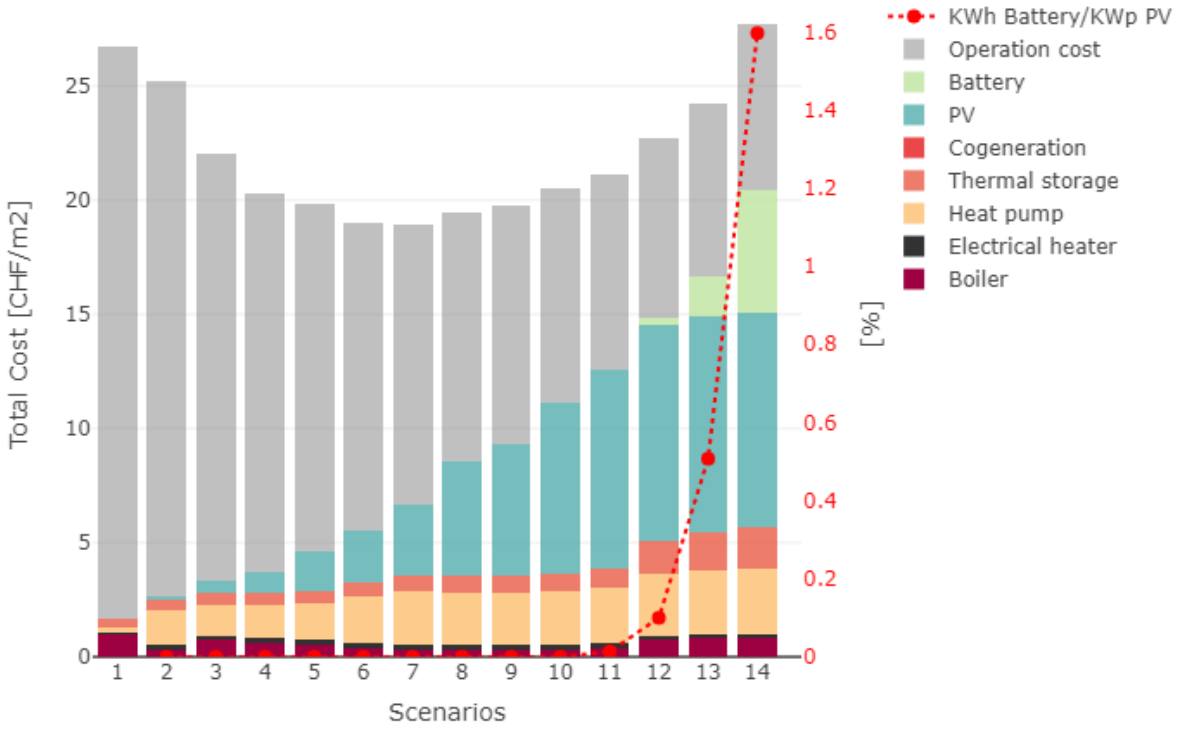

Figure 8: Operation and investment cost of equipment at district scale for each scenario without cogeneration.

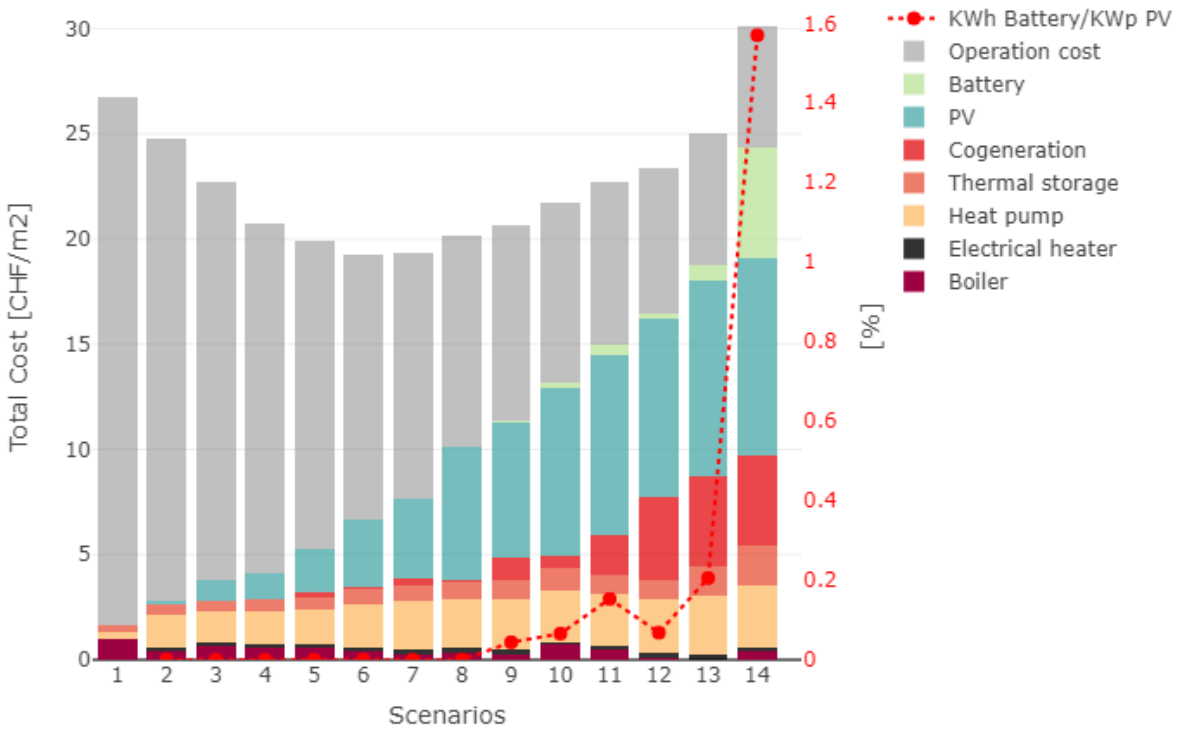

Figure 9: Operation and investment cost of equipment at district scale for each scenario with cogeneration.

The Figures 10 and 11 shows the annual electricity balance and the gas import at district scale for each optimal district-scale scenario with increasing self-sufficiency ratio.

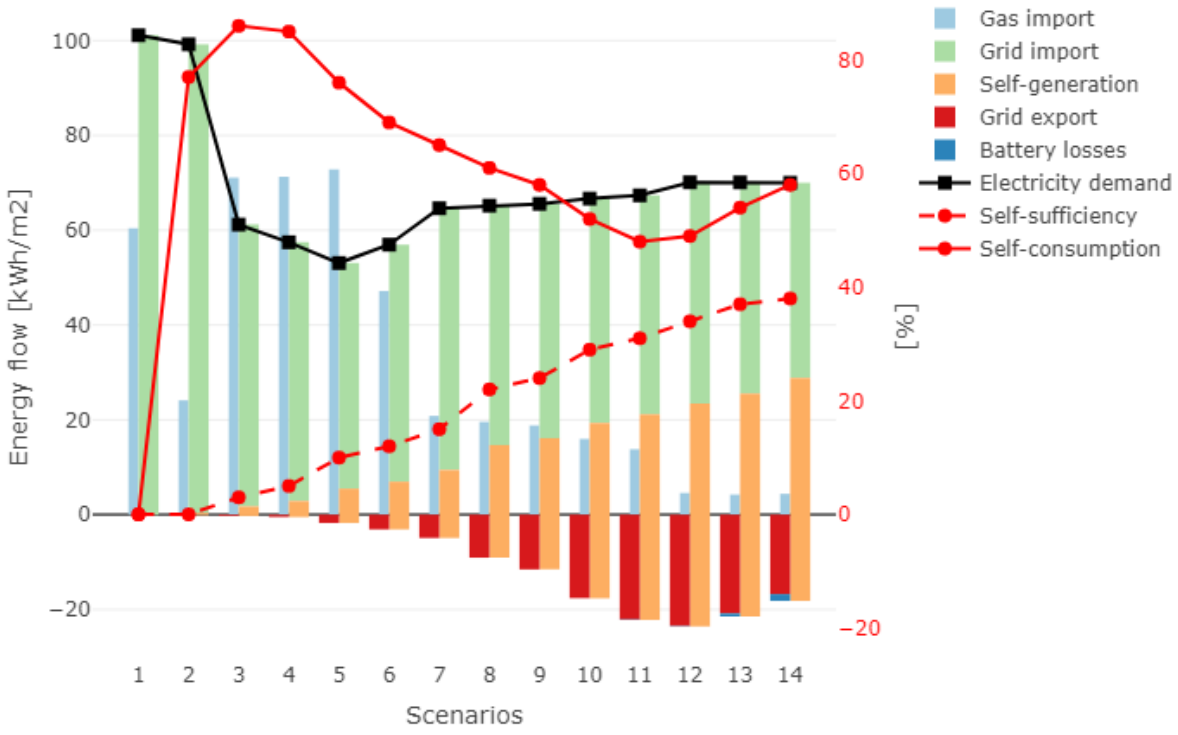

Figure 10: Energy flows at district scale for each scenarios without cogeneration.

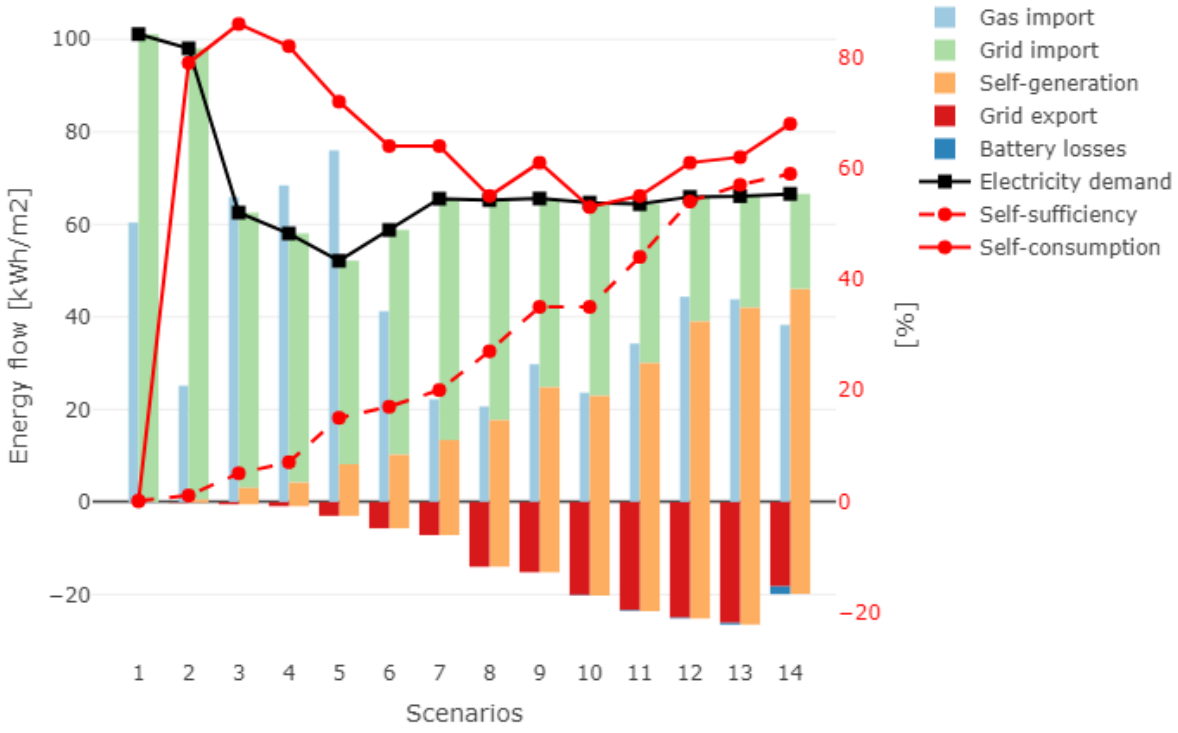

Figure 11: Energy flows at district scale for each scenarios with cogeneration.

4.2. Impact on the low voltage grid

A power flow solver [38] is applied on the fourteen optimal district-scale scenarios (§3.2) to calculate the voltage magnitude at the injection bus and the line current. For simplicity, we consider here only the case without cogeneration as it is the most grid intensive case. First, we analyze the impact of the technology scenario on the maximum voltage. Then the line loading level will be presented, and finally, the load-duration curve will be analyzed.

With the increasing PV penetration and the addition of self-generation technology (scenario 3 to 14), the maximum voltage magnitude (figure 12a) increases to value up to 1.06 p.u. This highlights a local excess of energy. The only increasing PV penetration is not the only factor. The addition of batteries that may all discharge at the same time can also significantly increase the voltage deviation. The minimum voltage magnitude, figure 12b show differents trends that come from the technology scenario. With the addition of PV, the minimum voltage magnitude increase (scenario 1 to 4), showing that the self-consumption of PV energy helps to compensate for the local deficit of energy. The moderate addition of heat pumps and electrical heaters has little effect on the minimum voltage but slightly increase local energy deficit, reducing voltage magnitude (scenario 5 to 11). The large drop in minimum voltage of scenario 12 to 14 can be explained by the addition of battery capacity, that will create, as they have synchronized charging patterns, heavy stress on the grid.

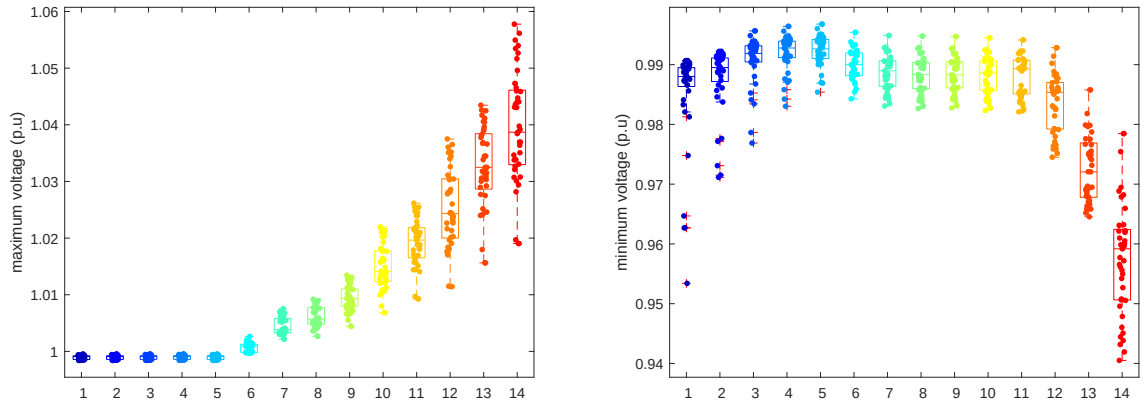

(a) Maximum bus voltage. *(b) Minimum bus voltage.*

Figure 12: Bus voltage extreme for each scenario.

Figure 13 illustrates the line loading perspective. On the left side (figure 13a shows the percentile 95 of the line loading level and indicates that future technology mix, with increasing PV penetration, will significantly reduce the current in the line 95% of the time. However, the maximum line loading level (figure 13b) on the right side, shows that the addition of PV and

batteries can increase the maximum current flowing through some particularly sensitive lines. This is especially true for scenarios 12 to 14, where the line loading increases again to reach similar values than scenarios 1 to 3. In this case, the addition of advanced technologies in the grid provides limited grid services.

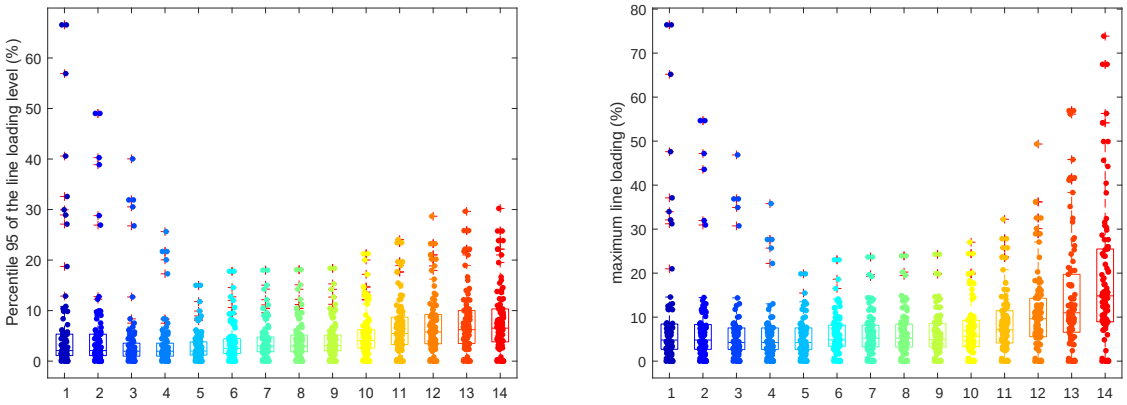

(a) Percentile 95 of the line loading level. *(b) Maximum line loading.*

Figure 13: Line loading for each scenario.

Finally, the load-duration curve illustrated in figure 20 highlights three distinct cases. First, from scenarios 1 to 3, the system relies heavily on the supplied power from the higher grid level (negative values indicate power flowing from the medium down to the low-voltage grid). Scenarios 4 to 10, where the addition of PV, heat pumps, and in a moderate measure, batteries, significantly reduce the energy dependency of the low-voltage grid on the higher grid level. The number of hours in which the grid has an excess of energy increases. Finally, the 3rd case occurs between scenario 11 to 14, where the high penetration of PV and batteries increase the transformer loading to much higher values (positive and negative).

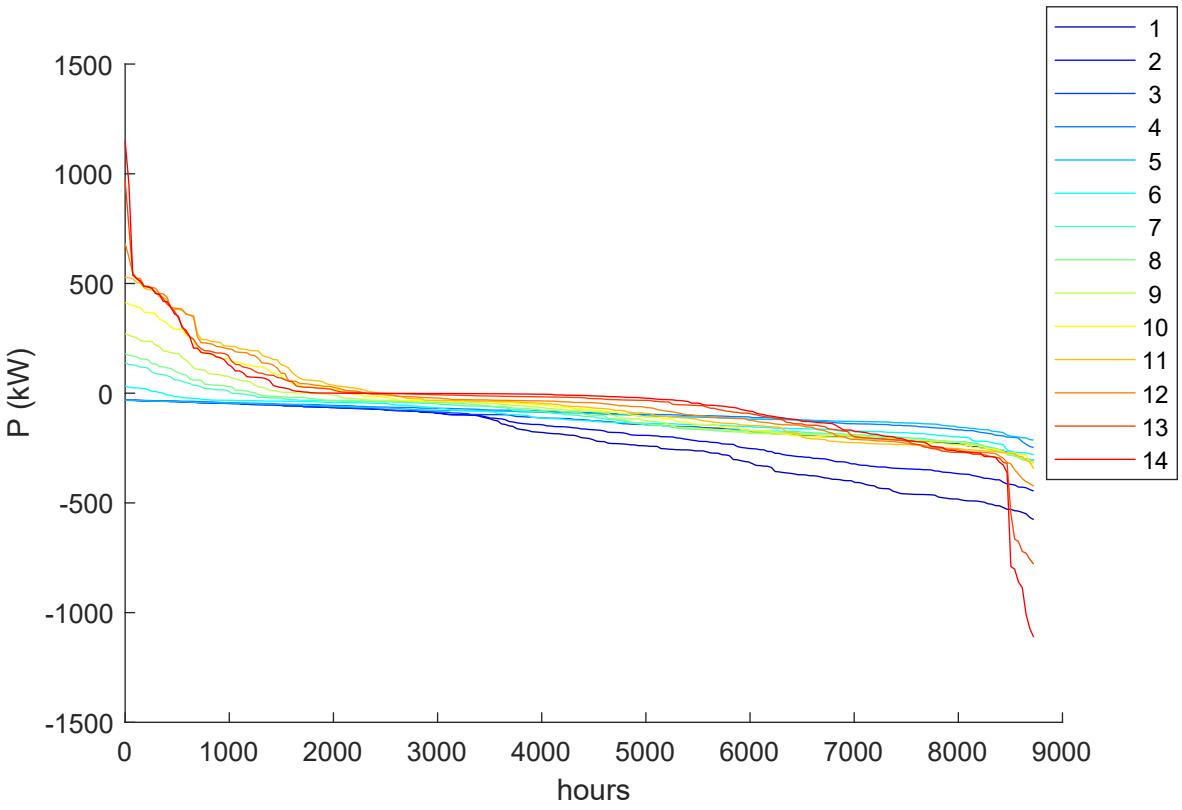

Figure 14: Load duration curve for each scenario.

This analysis highlights that future loads that depend on technology mix have the potential to reduce the gird's stress if selected carefully. A high PV and battery penetration may have a detrimental effect on the grid if no counter-measures are used. The following will show that grid tariffs can be used as grid services to mitigate the impact of high penetration of PV and batteries on the grid.

4.3. Mitigation impact of distributed PV with alternative electricity tariffs

The optimizations of the 41 buildings were performed on a Intel(R) Xeon(R) CPU E5-2630 v3 @ 2.40GHz processor with 8 Cores and 32GB of RAM using GUROBI[12] to solve the mixed-integer-linear problem. The power flows were then solved for each time step with a resolution of 15 min using PANDAPOWER [38].

Design and operation of the PV-battery energy systems

The resulting designs are pictured in Fig. 15. In all scenarios except the block rate tariff, almost all the roofs are covered with PV leading to a PV host value close to one. The block rate scenario, however, limits the penetration of PV. Regarding battery size, investment in such technology is driven by economic opportunities, namely by variations in the electricity price (solar and spot

market tariff scenarios) or by a strong incentive to limit the exchanged power (capacity tariff scenario). Although this last aspect is also present in the block rate scenario, the incentive is, thus, lower, leading to lower relative battery size. In terms of grid usage, only the capacity tariff and block rate tariff scenarios provide a clear incentive to reduce the maximum power exchanged with the grid. The spot market and solar tariff scenarios, due to the volatility of electricity prices, tend to increase the power injected or withdrawn from the grid. On the economic side, the discounted payback periods are similar, ranging from 14 to 23 years for all scenarios. The median is, however, higher for the block rate tariff, reaching 21 years against 19 years for the other scenarios.

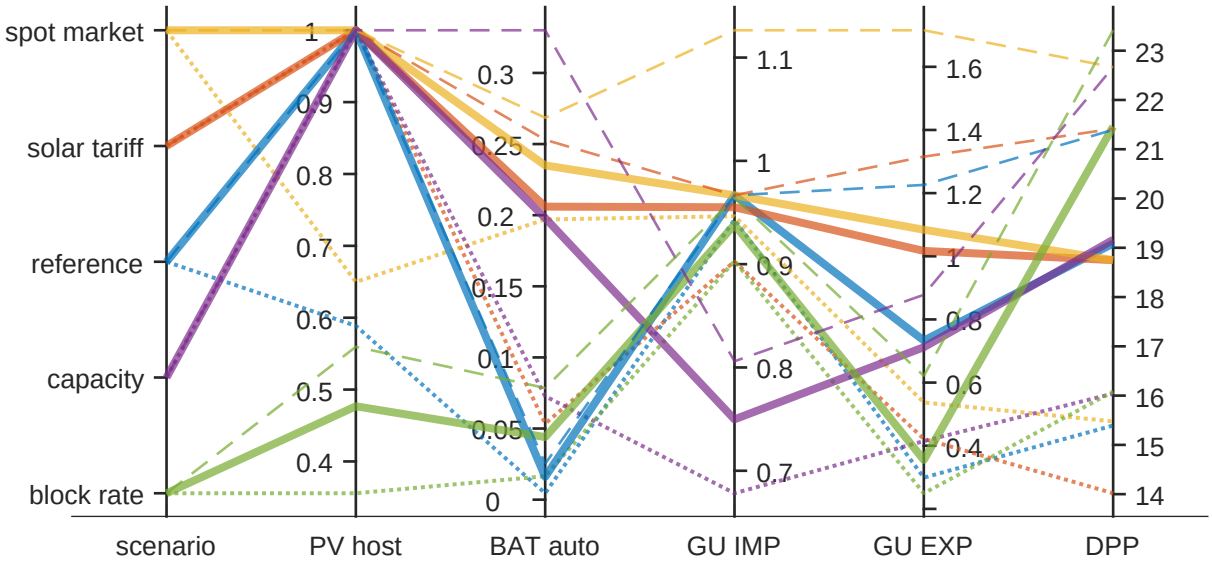

Figure 15: PV hosting ratio, battery autonomy, grid usage ratio (import/export) and discounted pay back period for all scenarios. Metrics are defined in (15)*. Solid lines are the median, dashed lines are the 75th percentile, and dotted lines are the 25th percentile.*

The relative size of the battery does not scale linearly with PV penetration, as depicted in Fig. 16, except for the dynamic volumetric tariffs (spot market and solar). For the capacity and block rate tariffs, low PV penetration, underlying a high consumption level compared to the PV production, tends to increase the battery autonomy ratio in order to limit the import power. Conversely, at high PV penetration, the battery autonomy tends to decrease for the capacity and block rate tariffs. For the first case, the role of the battery to cut injection peaks is replaced by the curtailment of the PV generation (Fig. 18). As curtailing is free, there is no need to invest in batteries for this purpose. For the block rate scenario, high injection is not penalized; the marginal revenue is just decreased. Thus, it limits the profitability of having a high PV capacity compared to its consumption level, but does not require either curtailment of the PV energy or investing in storage technologies. The fraction of energy curtailed is zero for all scenarios except the capacity and spot market tariffs. For the latter, the small fraction of curtailed energy

is due to negative spot market prices as shown in the inset of Fig. 18. As a general trend, a larger battery size relative to the building consumption increases the self-sufficiency ratio as shown in Fig. 17. This trend is very pronounced for the spot market, solar and capacity tariffs, although a saturation appears for the latter.

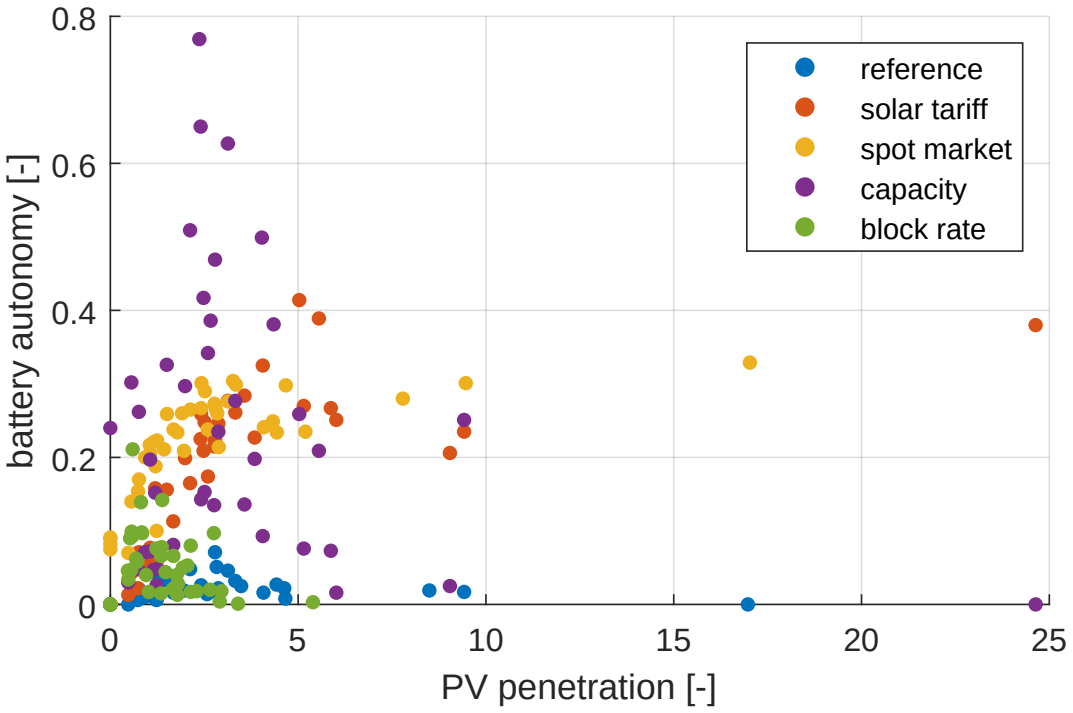

Figure 16: Battery autonomy versus PV penetration.

In summary, compared to the reference scenario, dynamic volumetric tariffs (solar and spot market) promote investments in storage technologies since they provide economic opportunities to generate profit for the building owners. The capacity tariff promotes investment in storage, but the main function this is to reduce consumption peaks by curtailment. The block rate tariff promotes smaller PV penetration (thus, PV capacity) and battery capacity but achieves a self-sufficiency level similar to the reference case. As pictured in Fig. 15, these considerations have an impact on grid usage behavior. In particular, the grid usage ratios are higher (regardless when importing or exporting) for both the spot market and solar tariff. It is especially pronounced for the spot market case. Conversely, capacity tariffs significantly drop the grid usage ratio for import, while the block rate tariff reduces both. Fig. 19 illustrates these observations. This figure allows us to distinguish between three types of grid user: the exporters, who have a grid usage ratio for export above 1 and even reduce their import grid usage by covering their own consumption; the energy traders, who buy or sell energy to maximize their profit and who tend to keep to their grid usage ratio for import and export above 1 (if the grid usage for export is below 1 it means that their own consumption dominates their generation

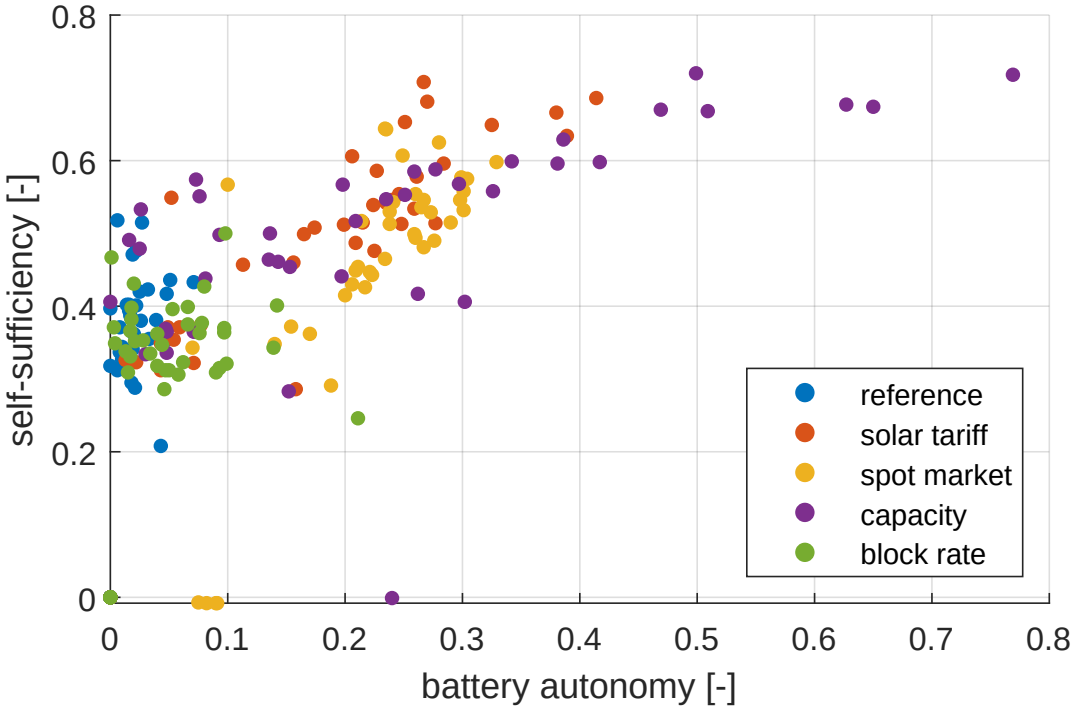

Figure 17: Self-sufficiency level against the battery autonomy ratio.

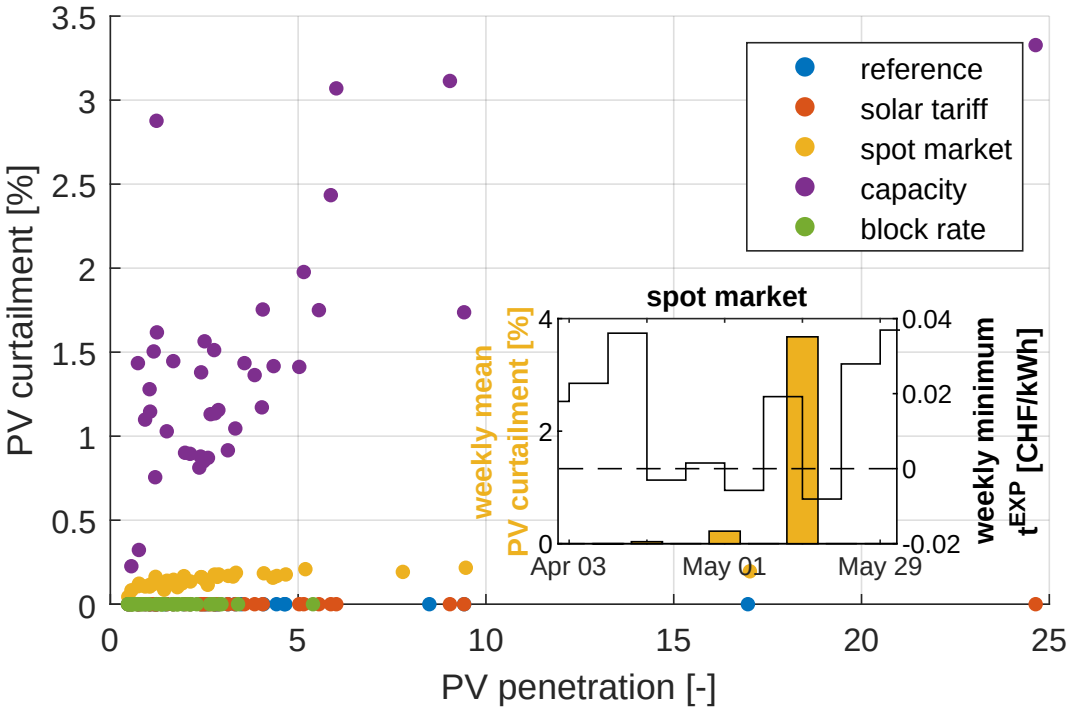

Figure 18: Ratio of energy curtailed and PV penetration. In the inset, the bars are the weekly ratio of energy curtailed (left axis) and lines the weekly minimum t^{EXP} (right axis).

capabilities); and the low grid users, who reduce both grid usage ratios, thus interacting less and less with the network. Almost all buildings fall in this category for the block rate scenario. The following will show how these local design and operation adaptations affect the network operational metrics.

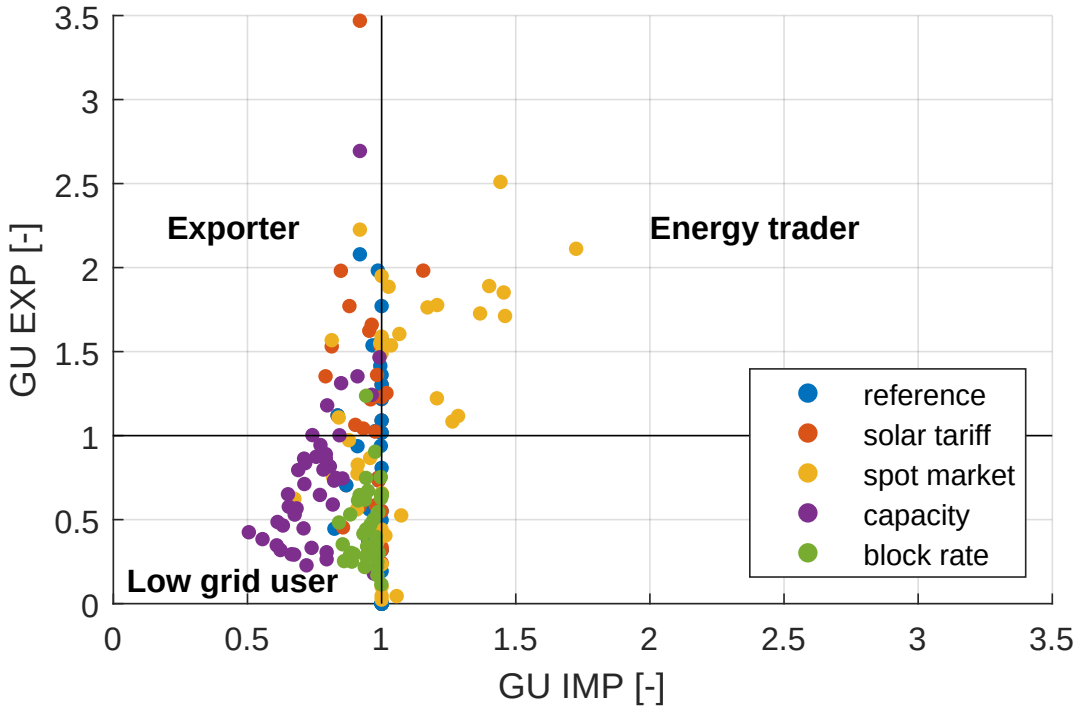

Figure 19: Export power ratio vs import power ratio.

Low-voltage grid impact

In order to have a complete overview of the grid reaction to the different tariff scenarios (in which PV installations and batteries are always present), two additional scenarios are added. The first considers only the original load without any investment in PV or batteries; the second considers that all roofs are covered with PV (regardless of the profitability of such a decision) but with no investment in batteries. These two scenarios set the upper and lower bounds to the grid impact metrics.

The load duration curve in Fig. 20 highlights the violation of the transformer power capacity for reverse power flow. All scenarios, except the load-only case, experience a maximum power flowing from the low-voltage side to the high-voltage side above 400 kW. The block rate, helped by a significantly lower installed PV capacity, has the lowest maximum reverse power, but a significant number of hours are above 400 kW. The most-demanding scenario is the spot market scenario which has the highest power demand and the highest injection power. The solar tariff also shows a significant increase in power demand compared to the other scenarios. This has

direct consequences for the level of loading of the lines (ratio between current and the maximum nominal current of the line). Fig. 21 shows that line loading level is significantly higher for all scenarios including PV, with the most extreme values attained under the spot market and full PV scenarios. The block rate tariff helps to significantly reduce the loading level of the lines. In this case, even the most loaded lines are less congested than in the load-only scenario.

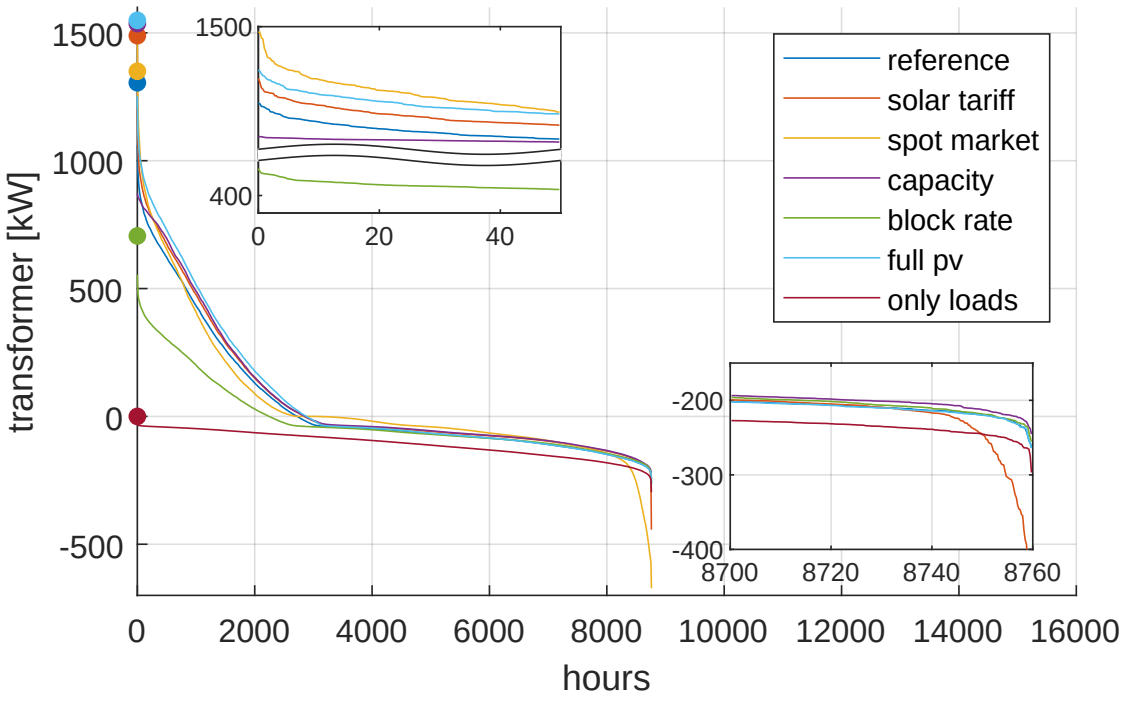

Figure 20: Load duration curve at the transformer. Dots on the vertical axis indicate the total installed PV capacity per scenario. The nominal transformer capacity is 400 kW. Negative values indicate power flow from the high-voltage toward the low-voltage side.

One of the main concerns of grid operators regarding high PV penetration is to keep voltage levels to a value as close as possible to 1 p.u. As a matter of fact, scenarios, except the spot market scenario, fulfill the criteria EN50160, meaning the voltage levels fall within +-10% of the nominal voltage for 95% of each week. When considering only the case when the voltage deviations exceed 1 p.u, Fig. 22 demonstrates the effectiveness of the capacity and block rate tariffs in terms of load management, as both lower the deviation of the most sensible bus compared to the reference and full PV case. Note that the load-only scenario is not displayed in this figure because the voltage levels never exceed 1 p.u. Alternatively, when the load level is below 1 p.u (Fig. 23), only the spot market case significantly increases the voltage deviations.

These observations highlight that advanced tariff structures can have two competing impacts. On the one hand, they help to mitigate the grid impact of distributed generation by promoting either small PV installations or moderate grid exchange. On the other hand, they can bring

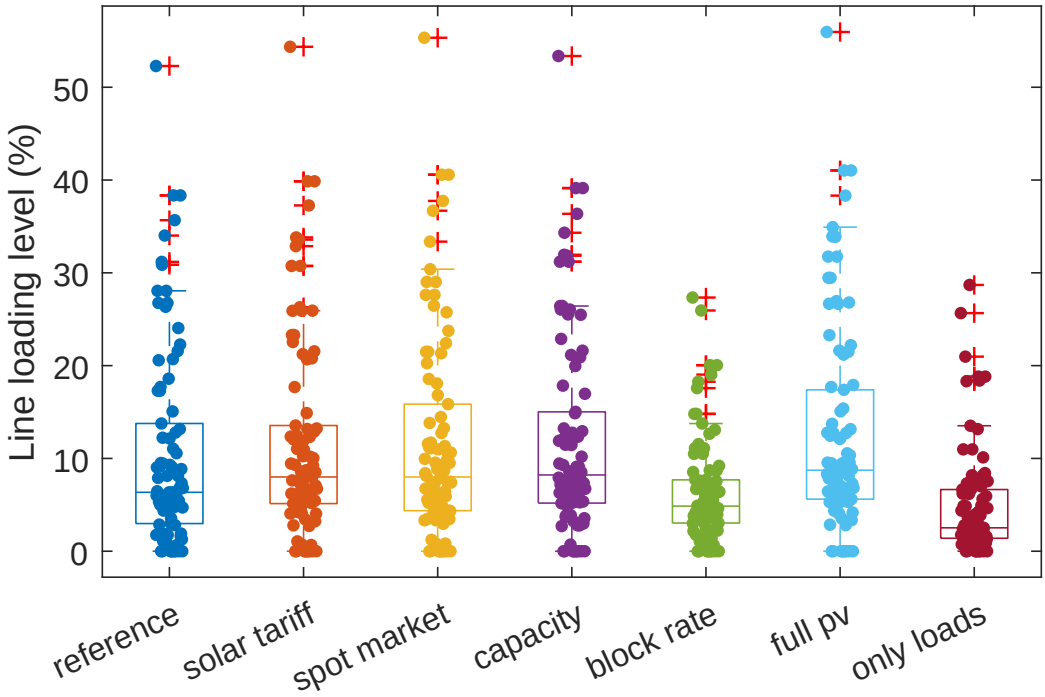

Figure 21: 95th percentile of the line loading level.

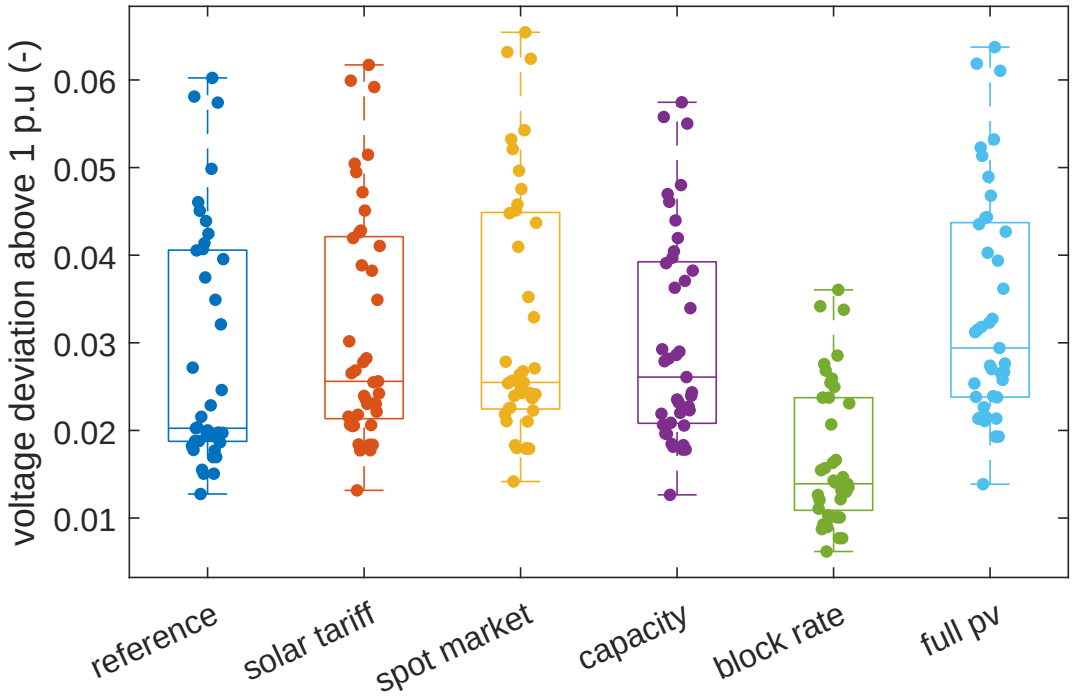

Figure 22: Voltage deviation distribution, when above 1 p.u

economic opportunities for significant investments in batteries and PV capacities but may in-

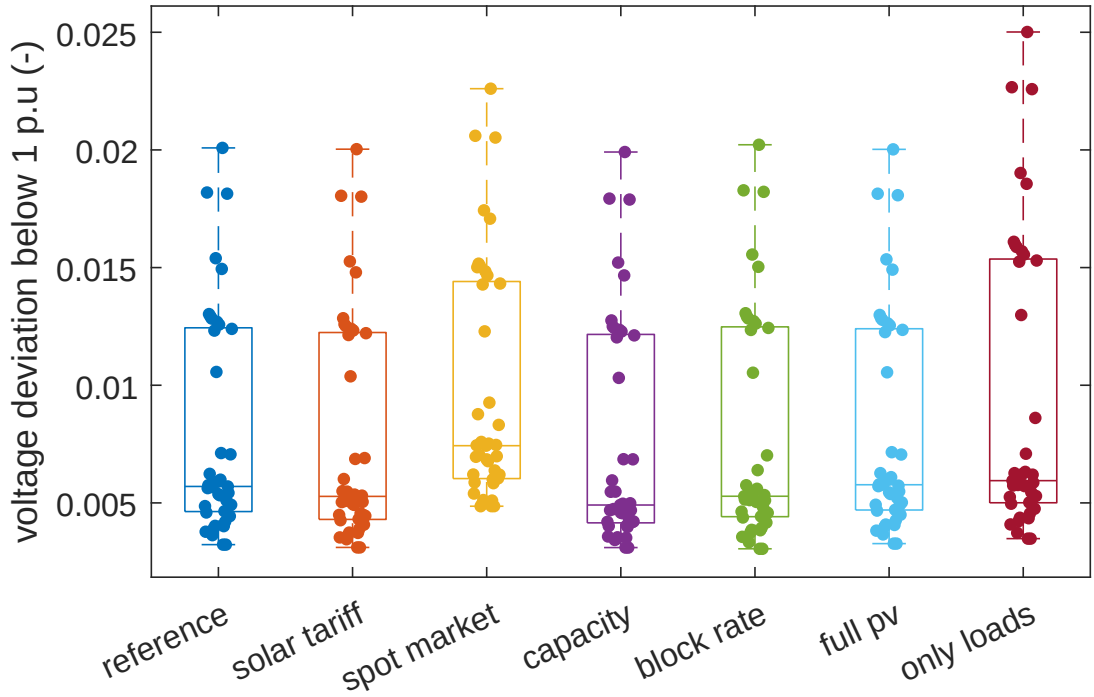

Figure 23: Voltage deviation distribution, when below 1 p.u

crease the pressure on the grid. The most-concerning aspect is the transformer capacity to bring the excess power from the low-voltage side to the upper level. Over/under-voltage and overloading of the lines are in this case far less concerning. Although each scenario has been carefully calibrated to globally keep the same total cost (with respect to the reference case) for all buildings, it is worth investigating the levelized cost of energy (LCOE) served in order to make sure that the resulting systems do not actually suffer from a net increase in the energy price.

Economic aspects

In the load-only scenario, the LCOE is 21 cts/kWh (corresponding to the import tariff of the reference scenario), while the LCOE can become higher in the full PV scenario, showing that an over-investment can occur and explaining why, in the reference case, some roofs are not covered with PV. Additionally, in the solar and spot market scenarios, only a small fraction of the buildings has an LCOE exceeding 21 cts/kWh, while the large majority would gain from switching to these tariff structures. For the capacity tariff scenario, a significant fraction of the buildings has an LCOE higher than the reference value, showing that, despite its positive impact on grid operation, such a tariff comes with a price for some building owners. The block rate scenario, though less prone for PV and battery investment, presents an LCOE lower than the reference values for all buildings. The design of such a tariff is a matter of compromise and

there is an apparent lack of literature for designing a block rate tariff in the specific scope of promoting distributed renewable energy and mitigating grid impact.

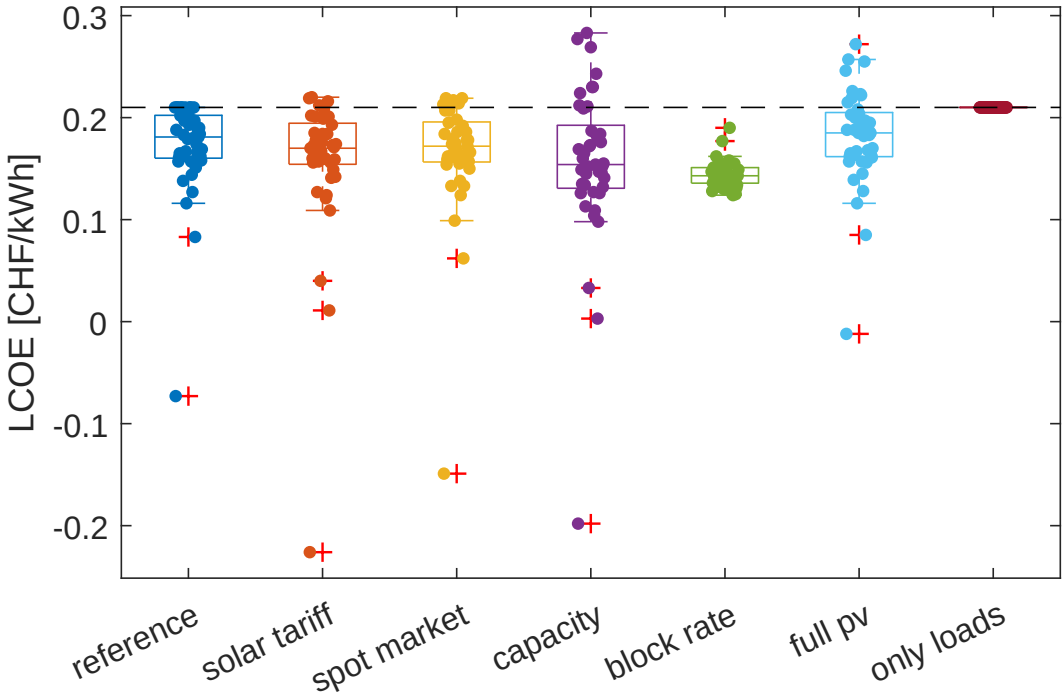

Figure 24: Levelized cost of energy per scenario.

Discussion

Our study performs the optimization of 41 buildings under five different tariff scenarios, including three volumetric tariffs, one combination of volumetric and capacity tariff and one block rate tariff. The resulting systems vary in term of installed PV capacity and battery capacity. The highest PV penetration is achieved with the capacity tariff while this scenario significantly reduces the voltage deviation and the line loading level. Volumetric tariffs, with high price volatility such as in the spot market scenario, lead to more investment and profitability of the batteries but also increase pressure on the network. Although the block rate scenario promotes smaller PV installation, it achieves the smallest median cost of providing energy for the end-users (from 18 cts/kWh in the reference case down to 14 cts/kWh). It reduces the 95th percentile of the positive voltage deviation of the bus with the larges deviation from 6% to 3.6% and reduces the maximum reverse power from 1060 kW to 550 kW, remaining above the 400 kW nominal power of the transformer. Further studies will elaborate on the design of block rate tariffs to mitigate network impact and incentivize high penetration of PV. The effect of a growing penetration of electric vehicles and heat pumps will also be considered.

4.4. Model predictive control (MPC)

The use of predictive control techniques (MPC), in contrast to standard rule-based approaches (RBC), significantly improves the integration of distributed generation units, showing an increase of as much as 27 percentage points in self-sufficiency for configurations with high PV penetration [34, 33]. Similarly, from an economic perspective, the rise in autonomy decreases the related operating expenses, particularly for larger, ill-sized distributed generation capacities (Figure 25).

Moreover, studies have confirmed that the use of a centralized predictive control approach to operate building energy system improves the community performances[26].

Finally, the use of a predictive model-based control method allows for the scheduling changes with respect to an initial demand profile, hence representing a virtual battery from the power network perspective (BES) [23].

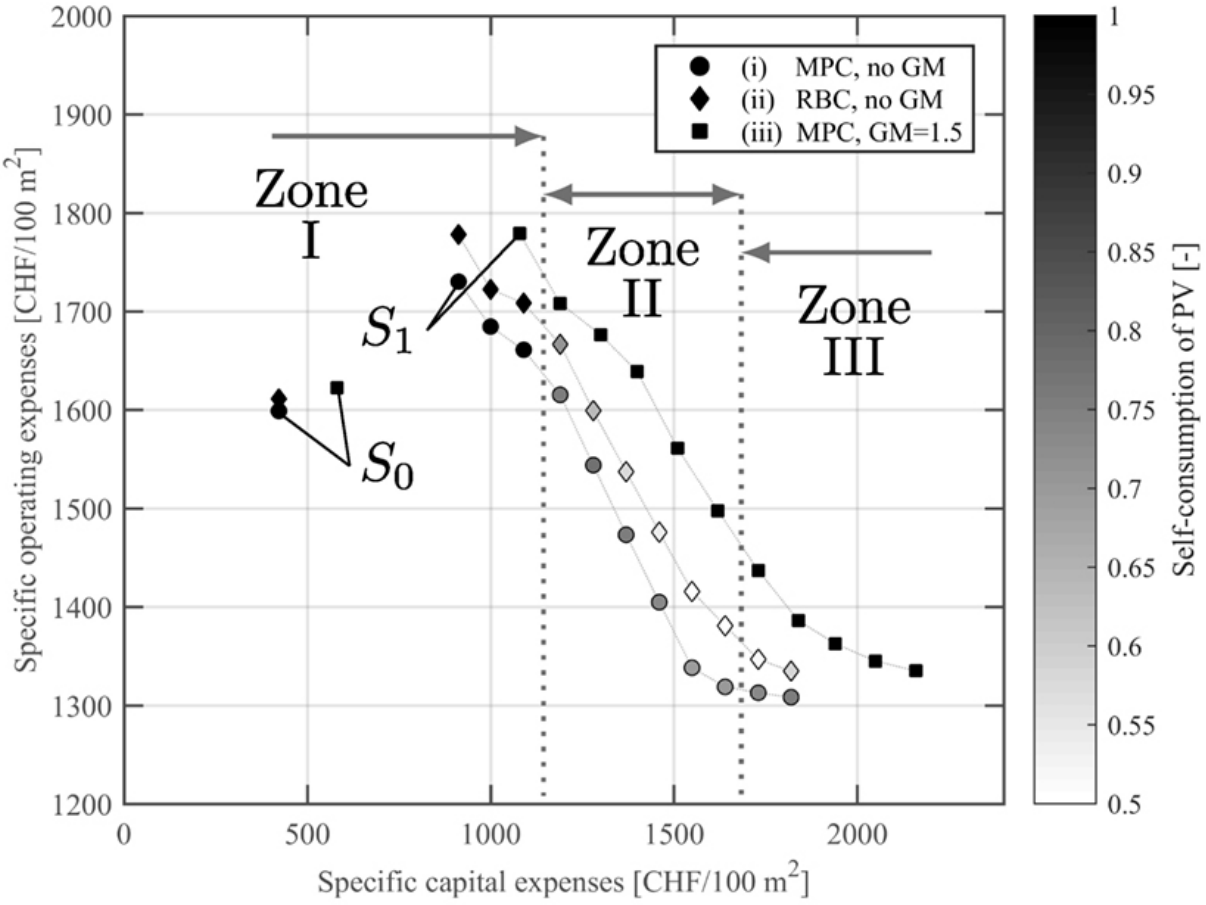

Figure 25: Pareto fronts for a single-family home when applying MPC (circles), RBC (diamonds), and MPC with a tight GM constraint (squares) - Source [34])

.

4.5. Load curtailment in the power grid

Figure 26 shows the effect on the load duration curve at transformer TR3716 of power curtailment done by the inverter. The current system is compared with two future scenarios, including photovoltaic pannels (PV), heat pumps (HP), batteries and cogeneration fuel cells (SOFC). Curtailment is obtained by forcing the grid multiple ratio of buildings (Equation 7) with a threshold value of ϵ_{GM}=2. This shows that the electrification of the district energy system with heat pumps, PV pannels and cogeneration engine requires the implementation of ancilliary services and/or investment in the transformer.

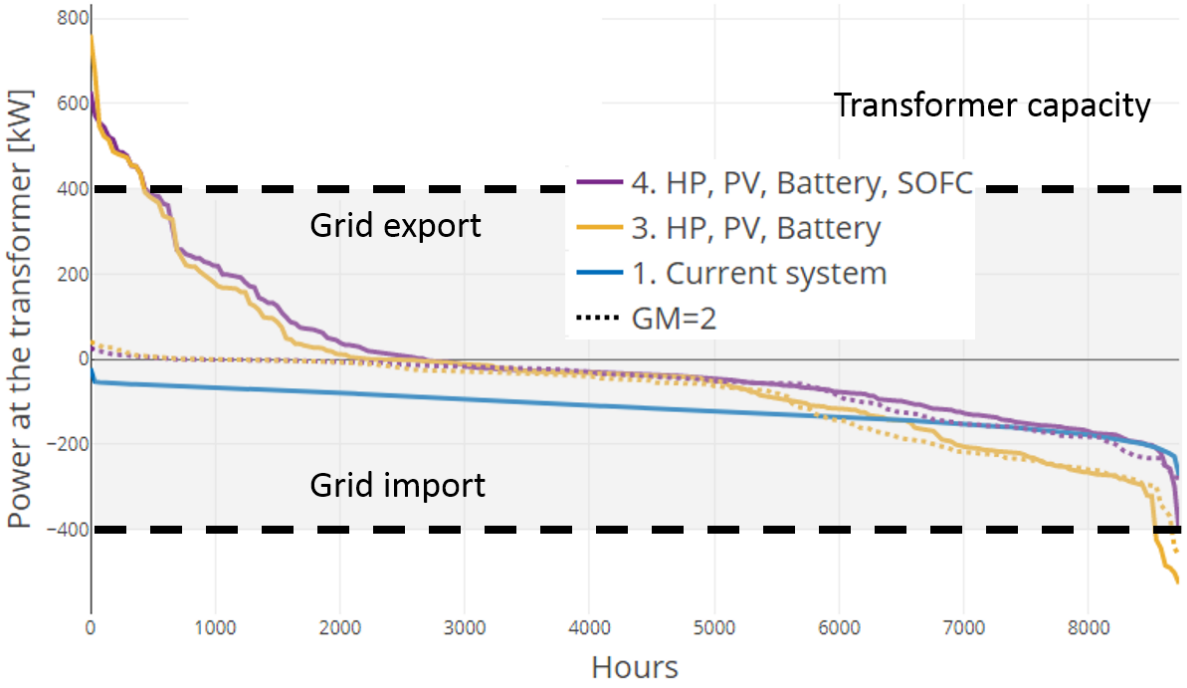

Figure 26: Load duration curve without (solid line) and with grid constraint (dotted lines) with a grid multiple of 2.

4.6. Building to district control MPC

The increase of performances of district-scale approach for multi-building energy system has been demonstrated by [26]. It is shown that, for the same services, better integration of distributed energy technologies can reduce the import from the grid from more than 15%. To achieve this performance, it is important not only to operate, but also to design equipment and storage at the district level (Figure 27). Simultaneously, applying district scale model predictive control reduces the operating expenses by 6-8% compared to building based control approach.

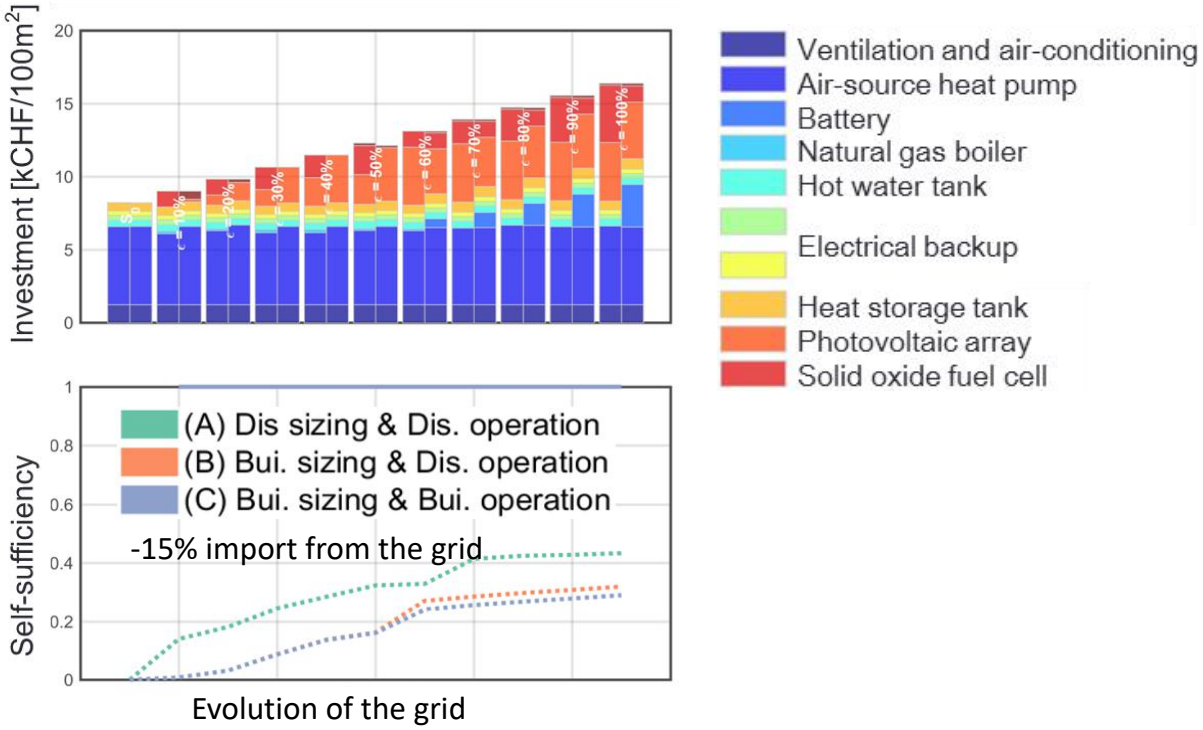

Figure 27: District versus building's scale MPC. Upper figure: investment in equipment when sized at buildings scale (left bars) and district scale (right bars). Lower figure: self-sufficiency when the same system is (C) designed and operated at building scale, (B) designed at building scale but operated at district scale, (A) designed and operated at district scale.

5. Conclusion

Based on an analysis of the possible ancillary services for the low voltage grid in line with building to district and district to grid approach, local automatic voltage control and centralized automatic voltage control have been identified as the most effective ancillary services for the RE Demo site. Therefore, advanced electricity tariff structures, model predictive control (MPC) at building scale, load constraints in the power grid and building to district control strategies have been implemented using multi-objective mixed integer linear programming (MILP) methods.

The method has been applied to forecast bus voltage, line loading and the load at district transformer for different energy system configurations with increasing self-sufficiency ratio.
The load-duration curve highlights three distinct cases: (i) the system relies heavily on the supplied power from the higher grid level (ii) the addition of PV, heat pumps, and in a moderate measure, batteries, significantly reduce the energy dependency of the low-voltage grid on the higher grid level (iii) the high penetration of PV and batteries creates a detrimental effect on the grid, highlighting the need for ancillary service in the grid.
The performances of the proposed ancillary services have been evaluated using a flow solver:

Advanced electricity tariff promotes smaller PV installation, it achieves the smallest median cost of providing energy for the end-users (from 18 cts/kWh in the reference case down to 14 cts/kWh). It reduces the 95th percentile of the positive voltage deviation of the bus with the larges deviation from 6% to 3.6% and reduces the maximum reverse power from 1060 kW to 550 kW, remaining above the 400 kW nominal power of the transformer.

Model predictive control in contrast to standard rule-based approaches (RBC), significantly improves the integration of distributed generation units, showing an increase of as much as 27 percentage points in self-sufficiency for configurations with high PV penetration.

Load curtailment constraints (grid multiple, usage and PV curtailment) have been implemented in the MPC strategy providing a mechanism to avoid overloading without grid reinforcement.

Building to district control can reduce the import from the grid from more than 15%. To achieve this performance, it is important not only to operate, but also to design equipment and storage at the district level.

As shown in previous applications [11], the implemented MILP-based algorithm can be deployed in control boxes developed using open-source standards, such as mikrobus[4].

[4] https://www.mikroe.com/mikrobus

References

[1] T. Beck, H. Kondziella, G. Huard, and T. Bruckner. Assessing the influence of the temporal resolution of electrical load and PV generation profiles on self-consumption and sizing of PV-battery systems. *Applied Energy*, 173:331–342, July 2016. https://doi.org/10.1016/j.apenergy.2016.04.050.

[2] Lionel Bloch, Jordan Holweger, Christophe Ballif, and Nicolas Wyrsch. Impact of advanced electricity tariff structures on the optimal design, operation and profitability of a grid-connected PV system with energy storage. *Energy Informatics*, 2(S1):1–19, 2019. https://doi.org/10.1186/s42162-019-0085-z.

[3] Lionel Bloch, Jordan Holweger, Nicolas Wyrsch, Hervé Tommasi, and Luc Girardin. Description of the multi-energy demonstration system in the re demo site , page 25, 2017.

[4] David H. Blum, Tea Zakula, and Leslie K. Norford. Opportunity Cost Quantification for Ancillary Services Provided by Heating, Ventilating, and Air-Conditioning Systems. *IEEE Transactions on Smart Grid*, 8(3):1264–1273, May 2017. https://doi.org/10.1109/TSG.2016.2582207.

[5] Christof Bucher, Jethro Betcke, and Goran Andersson. Effects of variation of temporal res-olution on domestic power and solar irradiance measurements. In *2013 IEEE Grenoble Conference*, pages 1–6, Grenoble, France, June 2013. IEEE. https://doi.org/10.1109/PTC.2013.6652217.

[6] Christoph Bucher. *Analysis and Simulation of Distribution Grids with Photovoltaics*. PhD thesis, ETH-Zürich, Zürich, 2014. https://doi.org/10.3929/ethz-a-010204387.

[7] Roel De Coninck and Lieve Helsen. Practical implementation and evaluation of model predictive control for an office building in Brussels. *Energy and Buildings*, 111:290–298, January 2016. https://doi.org/10.1016/j.enbuild.2015.11.014.

[8] Thomas A. Deetjen, J. Scott Vitter, Andrew S. Reimers, and Michael E. Webber. Optimal dispatch and equipment sizing of a residential central utility plant for improving rooftop solar integration. *Energy*, 147:1044–1059, March 2018. https://doi.org/10.1016/j.energy.2018.01.110.

[9] Stefan Deml, Andreas Ulbig, Theodor Borsche, and Goran Andersson. The role of aggregation in power system simulation. In *2015 IEEE Eindhoven PowerTech*, pages 1–6, Eindhoven, Netherlands, June 2015. IEEE. https://doi.org/10.1109/PTC.2015.7232755.

[10] R. Elsen, B. Aouini, Z. Barócsi, T. Bonnet, A. Bouzoualegh, H. J. Compter, J. Galindo, M. Gomes, C. Ioanitescu, and R. Jacquet. Ancillary Services Unbundling Electricity Products–an Emerging Market. *Union of the Electricity Industry–EURELECTRIC*, page 84, 2004.

[11] Luc Girardin, Paul Michael Stadler, and François Maréchal. Report on the role of multi-carrier, multi-services, multi-grids integrated energy conversion systems and their possible role in the swiss energy 2050 - deliverable d1.5.3., page 18, 2017. http://infoscience.epfl.ch/record/268355.

[12] LLC Gurobi Optimization. Gurobi optimizer reference manual, 2020. http://www.gurobi.com.

[13] Kai Heussen, Stephan Koch, Andreas Ulbig, and Goran Andersson. Energy storage in power system operation: The power nodes modeling framework. In *2010 IEEE PES Innovative Smart Grid Technologies Conference Europe (ISGT Europe)*, pages 1–8, Gothenburg, Sweden, October 2010. IEEE. https://doi.org/10.1109/ISGTEUROPE.2010.5638865.

[14] Kai Heussen, Stephan Koch, Andreas Ulbig, and Göran Andersson. Unified System-Level Modeling of Intermittent Renewable Energy Sources and Energy Storage for Power Sys-tem Operation. *IEEE Systems Journal*, 6(1):140–151, March 2012. https://doi.org/10. 1109/JSYST.2011.2163020.

[15] Christoph Hodel. Overview of ancillary services. Technical report, Swissgrid, 27 September 2019. version 1,1.

[16] Jordan Holweger, Lionel Bloch, Christophe Ballif, and Nicolas Wyrsch. Mitigating the impact of distributed PV in a low-voltage grid using electricity tariffs. *arXiv:1910.09807 [cs, eess]*, October 2019. https://arxiv.org/abs/1910.09807.

[17] IRENA. Global energy transformation: A roadmap to 2050. *International Renewable Energy Agency: Abu Dhabi*, page 76, 2018. https://www.irena.org/publications/2018/Apr/Global-Energy-Transition-A-Roadmap-to-2050.

[18] G. Joos, B. T. Ooi, D. McGillis, F. D. Galiana, and R. Marceau. The potential of distributed generation to provide ancillary services. In *2000 Power Engineering Society Summer Meeting (Cat. No.00CH37134)*, volume 3, pages 1762–1767 vol. 3, 2000. https: //doi.org/10.1109/PESS.2000.868792.

[19] Merla Kubli. Squaring the sunny circle? On balancing distributive justice of power grid costs and incentives for solar prosumers. *Energy Policy*, 114:173–188, March 2018. https: //doi.org/10.1016/j.enpol.2017.11.054.

[20] Luise Middelhauve, Lionel Bloch, and Luc Girardin. 5b design of sizes for build-ings energy systems as a function of the grid evolution - Technical report, EPFL Valais/ Neuchâtel, June 2018. https://infoscience.epfl.ch/record/ 268359?ln=fr.

[21] Rasmus Luthander, Joakim Widèn, Daniel Nilsson, and Jenny Palm. Photovoltaic self-consumption in buildings : A review. *Applied Energy*, 142:80–94, 2015. https://doi.org/10.1016/j.apenergy.2014.12.028.

[22] Rasmus Luthander, Joakim Widén, Daniel Nilsson, and Jenny Palm. Photovoltaic self-consumption in buildings: A review. *Applied Energy*, 142:80–94, March 2015. https: //doi.org/10.1016/j.apenergy.2014.12.028.

[23] Luise Middelhauve, Lionel Bloch, Jordan Holweger, Paul Michael Stadler, and Luc Girardin. 5d2 Detailed evaluation of the grid operation bottlenecks and load shifting potential for the reference system , 2019.

[24] Luise Middelhauve, Alessio Santeccia, Luc Girardin, Manuele Margni, and Francois Marechal. Key Performance Indicators for Decision Making in Building Energy Systems. *ECOS 2020 Proceedings*, page 12, 2020.

[25] Frauke Oldewurtel, David Sturzenegger, Goran Andersson, Manfred Morari, and Roy S. Smith. Towards a standardized building assessment for demand response. In *52nd IEEE Conference on Decision and Control*, pages 7083–7088, Firenze, December 2013. IEEE. https://doi.org/10.1109/CDC.2013.6761012.

[26] Stadler Paul. *Model-based sizing of building energy systems with renewable sources*. PhD thesis, EPFL, 2019. http://dx.doi.org/10.5075/epfl-thesis-9560.

[27] Yann G. Rebours, Daniel S. Kirschen, Marc Trotignon, and Sbastien Rossignol. A Survey of Frequency and Voltage Control Ancillary Services—Part I: Technical Features. *IEEE Transactions on Power Systems*, 22(1):350–357, February 2007. https://doi.org/10.1109/TPWRS.2006.888963.

[28] David Santos-Martin and Scott Lemon. Simplified Modeling of Low Voltage Distribution Networks for PV Voltage Impact Studies. *IEEE Transactions on Smart Grid*, 7(4):1924–1931, jul 2016. https://doi.org/10.1109/TSG.2015.2500620.

[29] Tim Schittekatte, Ilan Momber, and Leonardo Meeus. Future-proof tariff design: Recov-ering sunk grid costs in a world where consumers are pushing back. *Energy Economics*, 70:484–498, February 2018. https://doi.org/10.1016/j.eneco.2018.01.028.

[30] Michael Schreiber, Martin E. Wainstein, Patrick Hochloff, and Roger Dargaville. Flexible electricity tariffs: Power and energy price signals designed for a smarter grid. *Energy*, 93:2568–2581, December 2015. https://doi.org/10.1016/j.energy.2015.10.067.

[31] Paul Simshauser. Distribution network prices and solar PV: Resolving rate instability and wealth transfers through demand tariffs. *Energy Economics*, 54:108–122, February 2016. https://doi.org/10.1016/j.eneco.2015.11.011.

[32] Fabrizio Sossan. Equivalent electricity storage capacity of domestic thermostatically controlled loads. *Energy*, 122:767–778, March 2017. https://doi.org/10.1016/j.energy.2016.12.096.

[33] P. Stadler, L. Girardin, and F. Maréchal. The swiss potential of model predictive control for building energy systems. In *2017 IEEE PES Innovative Smart Grid Technologies Conference Europe (ISGT-Europe)*, pages 1–6, 2017. https://doi.org/10.1109/ISGTEurope.2017.8260100.

[34] Paul Stadler, Luc Girardin, Araz Ashouri, and François Maréchal. Contribution of Model Predictive Control in the Integration of Renewable Energy Sources within the Built Environment. *Frontiers in Energy Research*, 6, 2018. https://doi.org/10.3389/fenrg.2018.00022.

[35] Sebastian Stinner, Kristian Huchtemann, and Dirk Müller. Quantifying the operational flexibility of building energy systems with thermal energy storages. *Applied Energy*, 181:140–154, November 2016. https://doi.org/10.1016/j.apenergy.2016.08.055.

[36] swissgrid. Ancillary services. https://www.swissgrid.ch/en/home/operation/regulation/ancillary-services.html. Accessed: 2019-10-2.

[37] Orlando Talent and Haiping Du. Optimal sizing and energy scheduling of photovoltaic-battery systems under different tariff structures. *Renewable Energy*, 129:513–526, December 2018. https://doi.org/10.1016/j.renene.2018.06.016.

[38] L. Thurner, A. Scheidler, F. Schäfer, J. Menke, J. Dollichon, F. Meier, S. Meinecke, and M. Braun. pandapower — an open-source python tool for convenient modeling, analysis, and optimization of electric power systems. *IEEE Transactions on Power Systems*, 33(6):6510–6521, Nov 2018. https://doi.org/10.1109/TPWRS.2018.2829021.

[39] R. Tonkoski, D. Turcotte, and T. H.M. El-Fouly. Impact of high PV penetration on voltage profiles in residential neighborhoods. *IEEE Transactions on Sustainable Energy*, 3(3):518–527, jul 2012. https://doi.org/10.1109/TSTE.2012.2191425.

[40] Andreas Ulbig and Göran Andersson. Analyzing operational flexibility of electric power systems. *International Journal of Electrical Power & Energy Systems*, 72:155–164, November 2015. https://doi.org/10.1016/j.ijepes.2015.02.028.

[41] E. Union. Directive 2009/72/ec of the european parliament and of the council of 13 july 2009 concerning common rules for the internal market in electricity and repealing directive 2003/54/ec. *Off. J. Eur. Union L*, 211:55–93, 2009. https://eur-lex.europa.eu/eli/dir/2009/72/oj.